Supplementary Information

Novel Bipyrazolo[1,5-*a*]pyridine Luminogens with Aggregation-Induced Emission Enhancement Properties

Pu-Yen Hsiao and Jean-Ho Chu*

Department of Applied Science, National Taitung University, Taitung, Taiwan 95092

E-mail: j_hchu@nttu.edu.tw

Table of Contents

Preparation of starting substrates 1:

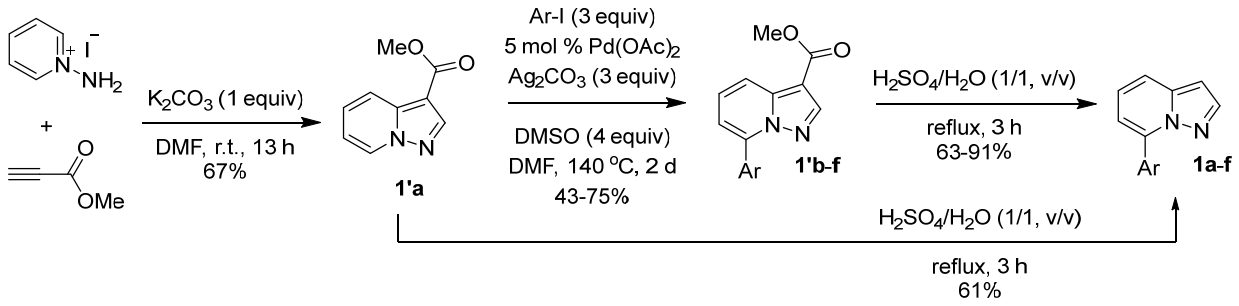

A solution of 1-aminopyridinium iodide (2.22 g, 10.0 mmol) and potassium carbonate (1.38 g, 10.0 mmol) in *N*,*N*-dimethylformamide (20 mL) was well stirred for 15 min at room temperature. Methyl propiolate (895 μL, 11.0 mmol) was next added into the above solution and the reaction was further stirred for 13 h. The solution was added with 100 mL of water and extracted with ethyl acetate (20 mL) for three runs. Combine the organic layers and the organic solution was washed with 50 mL of saturated NaCl (aq), dried over anhydrous $MgSO_4$, filtered through a pad of Celite, and evaporated *in vacuum*. The residue was dissolved in 10 mL of *n*-hexane/ethyl acetate (30/1, v/v), and underwent subsequent recrystallisation and flash chromatography using *n*-hexane/ethyl acetate (10/1 to 5/1) as the eluent to afford compound **1′a** in 67% yield (1.18 g, 6.70 mmol).

Next, a well-stirred solution of **1′a** (200 mg, 1.20 mmol), $Pd(OAc)_2$ (12.7 mg, 0.0566 mmol), and Ag_2CO_3 (939 mg, 3.59 mmol) in *N*,*N*-dimethylformamide (5 mL) was added with both dimethyl sulfoxide (325 μL, 4.54 mmol) and aryl iodide (3.6 mmol) at ambient temperature. The above solution was heated to 140 °C and stirred for 48 h. After cooling down to room temperature, 50 mL of water was added to the reaction and the solution was extracted by ethyl acetate (20 mL) for three runs. Subsequently, the organic layers were combined, dried over anhydrous $MgSO_4$, filtered through a pad of Celite, and evaporated *in vacuum*. The residue was further purified by flash chromatography using *n*-hexane/ethyl acetate (15/1 to 1/1) as the eluent to afford compound **1′b-f**, whose product yields are listed as follows. 72% of **1′b** (218 mg, 0.864 mmol), 75% of **1′c** (239 mg, 0.900 mmol), 70% of **1′d** (237 mg, 0.840 mmol), 65% of **1′e** (211 mg, 0.780 mmol), and 43% of **1′f** (131 mg, 0.516 mmol).

Finally, a well-stirred solution of **1′a-f** (0.20 mmol) in 2 mL of H_2SO_4/H_2O (1/1, v/v) was

heated under reflux (110 ºC) for 3 h. The solution was cooled down to room temperature and was neutralised with 1.0 M NaOH (aq) using litmus paper as the indicator. Then, 40 mL of water was added to the above solution and it was extracted by ethyl acetate (15 mL × 3). Organic layers were combined, dried over anhydrous $MgSO_4$, filtered through a pad of Celite, and evaporated *in vacuum*. The residue was purified by flash chromatography using *n*-hexane/ethyl acetate (25/1 to 3/2, v/v) as the eluent to afford compound **1a-f**, whose product yields are listed as follows. 61% of **1a** (14.3 mg, 0.122 mmol), 88% of **1b** (34.1 mg, 0.176 mmol), 91% of **1c** (37.9 mg, 0.182 mmol), 63% of **1d** (28.2 mg, 0.126 mmol), 77% of **1e** (32.6 mg, 0.154 mmol), 69% of **1f** (36.7 mg, 0.138 mmol).

Synthesis of 3,3′-bipyrazolo[1,5-*a*]pyridines (2a) and 7,7′-diaryl-3,3′-bipyrazolo[1,5-*a*]-pyridines (2b-f):

A solution of **1a-f** (0.20 mmol), $Pd(OAc)_2$ (4.6 mg, 0.020 mmol), and AgOAc (34 mg, 0.20 mmol) in dimethyl sulfoxide (4 mL) under N_2 atmosphere was well stirred and heated at 50 ºC overnight. After cooling down to room temperature, 20 mL of water was added to the above solution and which was extracted by ethyl acetate (15 mL × 3). The organic layers were next combined, treated by saturated NaCl (aq), dried over anhydrous $MgSO_4$, filtered through a pad of Celite, and evaporated *in vacuum*. Finally, the residue was purified by flash chromatography using *n*-hexane/dichloromethane/ethyl acetate (1/1/0 to 30/30/7, v/v/v) as the eluent to afford compounds **2a-f**. The amounts used of **1** and product yields of **2** are listed as follows. **1a**: 24 mg for 35% of **2a** (8.2 mg, 0.035 mmol), **1b**: 38 mg for 50% of **2b** (19 mg, 0.050 mmol), **1c**: 42 mg for 50% of **2c** (21 mg, 0.050 mmol), **1d**: 44 mg for 54% of **2d** (24 mg, 0.054 mmol), **1e**: 42 mg for 55% of **2e** (23 mg, 0.055 mmol), and **1f**: 44 mg for 62% of **2f** (30 mg, 0.062 mmol).

Characterisation data of compounds 1 and 2:

Pyrazolo[1,5-*a*]pyridine (1a):[1] It was obtained as a pale-brown viscous liquid in 61% isolated yield; R_f = 0.51 (*n*-Hexane/Ethyl acetate = 1/1, v/v); ^{1}H NMR (400 MHz, $CDCl_3$) δ 8.47 (d, J = 7.2 Hz, 1 H), 7.94 (s, 1 H), 7.53 (d, J = 8.8 Hz, 1 H), 7.08 (t, J = 6.8 Hz, 1 H), 6.74 (t, J = 8.0 Hz, 1 H), 6.50 (s, 1 H); MS (EI) *m/z* 118 (M^+, 100).

7-Phenylpyrazolo[1,5-*a*]pyridine (1b):[2] It was obtained as a pale-yellow viscous liquid in 88% isolated yield; R_f = 0.49 (*n*-Hexane/Ethyl acetate = 10/1, v/v); ^{1}H NMR (400 MHz, $CDCl_3$) δ 7.96 (d, J = 2.4 Hz, 1 H), 7.85 (d, J = 7.6 Hz, 2 H), 7.49-7.40 (m, 4 H), 7.07 (dd, J = 8.8, 7.2 Hz, 1 H), 6.73 (dd, J = 7.2, 0.8 Hz, 1 H), 6.55 (d, J = 2.0 Hz, 1 H); MS (EI) *m/z* 194 (M^+, 69), 193 (100), 51 (51).

7-(*p*-Tolyl)pyrazolo[1,5-*a*]pyridine (1c): It was obtained as a pale-yellow viscous liquid in 91% isolated yield; R_f = 0.54 (*n*-Hexane/Ethyl acetate = 8/1, v/v); ^{1}H NMR (400 MHz, $CDCl_3$) δ 7.97 (d, J = 2.4 Hz, 1 H), 7.77 (d, J = 8.0 Hz, 2 H), 7.53 (dd, J = 8.8, 1.2 Hz, 1 H), 7.32 (d, J = 7.6 Hz, 2 H), 7.17 (dd, J = 8.8, 7.2 Hz, 1 H), 6.79 (dd, J = 6.8, 1.2 Hz, 1 H), 6.59 (d, J = 1.6 Hz, 1 H), 2.43 (s, 3 H); ^{13}C{^{1}H} NMR (101 MHz, $CDCl_3$) δ 141.3 (CH), 141.2 (Cq), 140.7 (Cq), 139.4 (Cq), 130.9 (Cq), 129.1 (CH × 2), 129.0 (CH × 2), 123.4 (CH), 116.8 (CH), 112.1 (CH), 97.0 (CH), 21.4 (CH_3); HRMS (ESI-TOF) *m/z*: $[M + H]^+$ calcd for $C_{14}H_{14}N_2$ 209.1079; Found 209.1080.

7-(*p*-Methoxyphenyl)pyrazolo[1,5-*a*]pyridine (1d):[2] It was obtained as a white solid in 63% isolated yield; mp 92–93 ºC; R_f = 0.51 (*n*-Hexane/Ethyl acetate = 5/1, v/v); ^{1}H NMR (400 MHz, $CDCl_3$) δ 7.97 (d, J = 2.2 Hz, 1 H), 7.85 (d, J = 8.8 Hz, 2 H), 7.52 (dd, J = 8.8, 1.2 Hz, 1 H), 7.16 (dd, J = 8.8, 7.2 Hz, 1 H), 7.05 (d, J = 8.8 Hz, 2 H), 6.78 (dd, J = 6.9, 1.2 Hz, 1 H), 6.59 (d, J = 2.4 Hz, 1 H), 3.88 (s, 3 H); MS (EI) *m/z* 224 (M^+, 100).

7-(*p*-Fluorophenyl)pyrazolo[1,5-a]pyridine (1e): It was obtained as a pale-yellow viscous liquid in 77% isolated yield; R_f = 0.53 (*n*-Hexane/Ethyl acetate = 10/1, v/v); ^{1}H NMR (400 MHz, $CDCl_3$)

δ 7.98 (d, J = 2.4 Hz, 1 H), 7.91–7.87 (m, 2 H), 7.56 (d, J = 8.8 Hz, 1 H), 7.23–7.16 (m, 3 H), 6.78 (d, J = 6.8 Hz, 1 H), 6.62 (d, J = 2.4 Hz, 1 H); $^{13}C\{^{1}H\}$ NMR (101 MHz, $CDCl_3$) δ 163.2 (d, $J_{C\text{-}F}$ = 248.0 Hz, Cq), 141.4 (CH), 141.2 (Cq), 139.6 (Cq), 131.1 (d, $J_{C\text{-}F}$ = 8.0 Hz, CH × 2), 129.8 (d, $J_{C\text{-}F}$ = 4.0 Hz, Cq), 123.3 (CH), 117.3 (CH), 115.5 (d, $J_{C\text{-}F}$ = 22.0 Hz, CH × 2), 112.4 (CH), 97.3 (CH); HRMS (EI-TOF) *m/z*: $[M]^+$ calcd for $C_{13}H_9FN_2$ 212.0750; Found 212.0747.

7-(1-Naphthyl)pyrazolo[1,5-*a*]pyridine (1f): It was obtained as a white solid in 69% isolated yield; mp 148–149 °C; R_f = 0.44 (*n*-Hexane/Ethyl acetate = 8/1, v/v); ^{1}H NMR (400 MHz, $CDCl_3$) δ 8.04 (s, 1 H), 7.98 (s, 1 H), 7.86 (d, J = 7.6 Hz, 1 H), 7.63–7.56 (m, 2 H), 7.40 (t, J = 8.0 Hz, 1 H), 7.18 (t, J = 8.8 Hz, 1 H), 6.81 (d, J = 8.4 Hz, 1 H), 6.62 (s, 1 H); $^{13}C\{^{1}H\}$ NMR (101 MHz, $CDCl_3$) δ 141.8 (CH), 140.9 (Cq), 139.6 (Cq), 133.6 (Cq), 131.9 (Cq), 1315. (Cq), 130.0 (CH), 128.5 (CH), 127.9 (CH), 126.6 (CH), 126.2 (CH), 125.4 (CH × 2), 123.1 (CH), 117.6 (CH), 113.9 (CH), 97.1 (CH); HRMS (EI-TOF) *m/z*: $[M]^+$ calcd for $C_{17}H_{12}N_2$ 244.1000; Found 244.1009.

3,3'-Bipyrazolo[1,5-*a*]pyridine (2a): It was obtained as a yellow solid in 35% isolated yield; mp 195–196 °C; R_f = 0.56 (*n*-Hexane/Ethyl acetate = 2/3, v/v); ^{1}H NMR (400 MHz, $CDCl_3$) δ 8.52 (d, J = 7.0 Hz, 2 H), 8.13 (s, 2 H), 7.61 (d, J = 8.9 Hz, 2 H), 7.15 (td, J = 8.9, 0.9 Hz, 2 H), 6.81 (td, J = 6.8, 1.0 Hz, 2 H); $^{13}C\{^{1}H\}$ NMR (101 MHz, $CDCl_3$) δ 140.4 (CH × 2), 137.5 (Cq × 2), 128.9 (CH × 2), 123.4 (CH × 2), 117.5 (CH × 2), 112.0 (CH × 2), 103.4 (Cq × 2); HRMS (EI-TOF) *m/z*: $[M]^+$ calcd for $C_{14}H_{10}N_4$ 234.0905; Found 234.0913.

7,7'-Diphenyl-3,3'-bipyrazolo[1,5-*a*]pyridine (2b): It was obtained as a yellow solid in 50% isolated yield; mp 193–194 °C; R_f = 0.47 (*n*-Hexane/Ethyl acetate = 4/1, v/v); ^{1}H NMR (400 MHz, $CDCl_3$) δ 8.19 (s, 2 H), 7.95-7.93 (m, 4 H), 7.64 (dd, J = 8.9, 1.1 Hz, 2 H), 7.59-7.49 (m, 6 H), 7.26 (dd, J = 6.9, 8.8 Hz, 2 H), 6.88 (dd, J = 6.8, 1.2 Hz, 2 H); $^{13}C\{^{1}H\}$ NMR (101 MHz, $CDCl_3$) δ 140.8 (Cq × 2), 140.2 (CH × 2), 138.7 (Cq × 2), 133.6 (Cq × 2), 129.5 (CH × 2), 129.2 (CH × 4), 128.5 (CH × 4), 116.4 (CH × 2), 112.9 (CH × 2), 103.8 (Cq × 2); HRMS (EI-TOF) *m/z*: $[M]^+$ calcd for

$C_{26}H_{18}N_4$ 386.1531; Found 386.1535.

7,7'-Di(*p*-tolyl)-3,3'-bipyrazolo[1,5-*a*]pyridine (2c): It was obtained as a yellow solid in 50% isolated yield; mp 230–231 °C; R_f = 0.51 (*n*-Hexane/Ethyl acetate = 4/1, v/v); ^{1}H NMR (400 MHz, $CDCl_3$) δ 8.17 (s, 2 H), 7.82 (d, J = 8.1 Hz, 4 H), 7.60 (d, J = 8.1 Hz, 2 H), 7.36 (d, J = 7.9 Hz, 4 H), 7.23 (dd, J = 8.8, 6.9 Hz, 2 H), 6.85 (d, J = 8.1 Hz, 2 H), 2.46 (s, 6 H); ^{13}C{^{1}H} NMR (101 MHz, $CDCl_3$) δ 141.1 (Cq × 2), 140.3 (CH × 2), 139.7 (Cq × 2), 138.8 (Cq × 2), 130.9 (Cq × 2), 129.3 (CH × 4), 129.2 (CH × 4), 123.8 (CH × 2), 116.3 (CH × 2), 112.7 (CH × 2), 103.9 (Cq × 2), 21.6 (CH_3 × 2); HRMS (EI-TOF) *m/z*: $[M]^+$ calcd for $C_{28}H_{22}N_4$ 414.1844; Found 414.1850.

7,7'-Di(*p*-methoxyphenyl)-3,3'-bipyrazolo[1,5-*a*]pyridine (2d): It was obtained as a yellow solid in 54% isolated yield; mp 235–236 °C; R_f = 0.46 (*n*-Hexane/Ethyl acetate = 3/1, v/v); ^{1}H NMR (400 MHz, $CDCl_3$) δ 8.17 (s, 2 H), 7.91 (d, J = 8.8 Hz, 4 H), 7.59 (dd, J = 8.8, 1.1 Hz, 2 H), 7.23 (dd, J = 8.8, 6.9 Hz, 2 H), 7.08 (d, J = 8.8 Hz, 4 H), 6.85 (dd, J = 6.9, 1.0 Hz, 2 H), 3.90 (s, 6 H); ^{13}C{^{1}H} NMR (101 MHz, $CDCl_3$) δ 160.5 (Cq × 2), 140.7 (Cq × 2), 140.1 (CH × 2), 138.7 (Cq × 2), 130.6 (CH × 4), 126.0 (Cq × 2), 123.7 (CH × 2), 115.9 (CH × 2), 114.0 (CH × 4), 112.3 (CH × 2), 103.8 (Cq × 2), 55.4 (CH_3 × 2); HRMS (ESI-TOF) *m/z*: $[M + H]^+$ calcd for $C_{28}H_{23}N_4O_2$ 447.1821; Found 447.1820.

7,7'-Di(*p*-fluorophenyl)-3,3'-bipyrazolo[1,5-*a*]pyridine (2e): It was obtained as a pale-yellow solid in 55% isolated yield; mp 261–262 °C; R_f = 0.48 (*n*-Hexane/Ethyl acetate = 4/1, v/v); ^{1}H NMR (400 MHz, $CDCl_3$) δ 8.17 (s, 2 H), 7.96-7.92 (m, 4 H), 7.63 (dd, J = 8.9, 1.2 Hz, 2 H), 7.27-7.22 (m, 6 H), 6.86 (dd, J = 6.9, 1.0 Hz, 2 H); ^{13}C{^{1}H} NMR (101 MHz, $CDCl_3$) δ 163.3 (d, $J_{C\text{-}F}$ = 248.0 Hz, Cq × 2), 140.2 (CH × 2), 139.8 (Cq × 2), 138.7 (Cq × 2), 131.2 (d, $J_{C\text{-}F}$ = 9.0 Hz, CH × 4), 129.6 (d, $J_{C\text{-}F}$ = 3.0 Hz, Cq × 2), 123.7 (CH × 2), 116.5 (CH × 2), 115.6 (d, $J_{C\text{-}F}$ = 22.0 Hz, CH × 4), 112.9 (CH × 2), 103.9 (Cq × 2); HRMS (EI-TOF) *m/z*: $[M]^+$ calcd for $C_{26}H_{16}F_2N_4$ 422.1343; Found 422.1349.

7,7'-Di(1-naphthyl)-3,3'-bipyrazolo[1,5-*a*]pyridine (2f): It was obtained as a pale-yellow solid in 62% isolated yield; mp 297–298 °C; R_f = 0.61 (*n*-Hexane/Ethyl acetate = 1/2, v/v); ^{1}H NMR (400 MHz, $CDCl_3$) δ 8.14 (s, 2 H), 8.04 (d, J = 8.1 Hz, 2 H), 7.96 (d, J = 8.3 Hz, 2 H), 7.78 (d, J = 9.0 Hz, 2 H), 7.72 (d, J = 6.4 Hz, 2 H), 7.65 (t, J = 8.0 Hz, 2 H), 7.53 (td, J = 6.0, 1.6 Hz, 2 H), 7.46-7.34 (m, 4 H), 7.32 (dd, J = 8.9, 6.8 Hz, 2 H), 6.92 (d, J = 6.8 Hz, 2 H); ^{13}C{^{1}H} NMR (101 MHz, $CDCl_3$) δ 140.5 (CH × 2), 139.8 (Cq × 2), 138.3 (Cq × 2), 133.6 (Cq × 2), 131.7 (Cq × 2), 131.4 (Cq × 2), 130.2 (CH × 2), 128.6 (CH × 2), 127.9 (CH × 2), 126.7 (CH × 2), 126.3 (CH × 2), 125.5 (CH × 2), 125.4 (CH × 2), 123.5 (CH × 2), 116.9 (CH × 2), 114.4 (CH × 2), 103.8 (Cq × 2); HRMS (EI-TOF) *m/z*: $[M]^+$ calcd for $C_{34}H_{22}N_4$ 486.1844; Found 486.1847.

Reference

1. Balkenhohl, M.; Salgues, B.; Hirai, T.; Karaghiosoff, K.; Knochel, P. *Org. Lett.* **2018**, *20*, 3114−3118.
2. Wu, H.-C.; Chu, J.-H.; Hwang, L.-C.; Wu, M.-J. *Organometallics* **2016**, *35*, 288−300.

Proposed catalytic mechanism:

First, the reaction of substrate **1** and palladium(II) acetate generates intermediate **I** *via* C(3)-H palladation by the release of HOAc. Subsequently, the palladium(II) centre of intermediate **I** activates the C(3′)-H bond of another substrate **1** to give intermediate **II** that accompanies the release of HOAc. Intermediate **II** next undergoes the reductive elimination step to afford the corresponding bipyrazolo[1,5-*a*]pyridines **2**. Finally, the released palladium(0) is oxidised and regenerates the palladium(II) by two equivalents of silver acetate, and continues the next catalytic cycle.

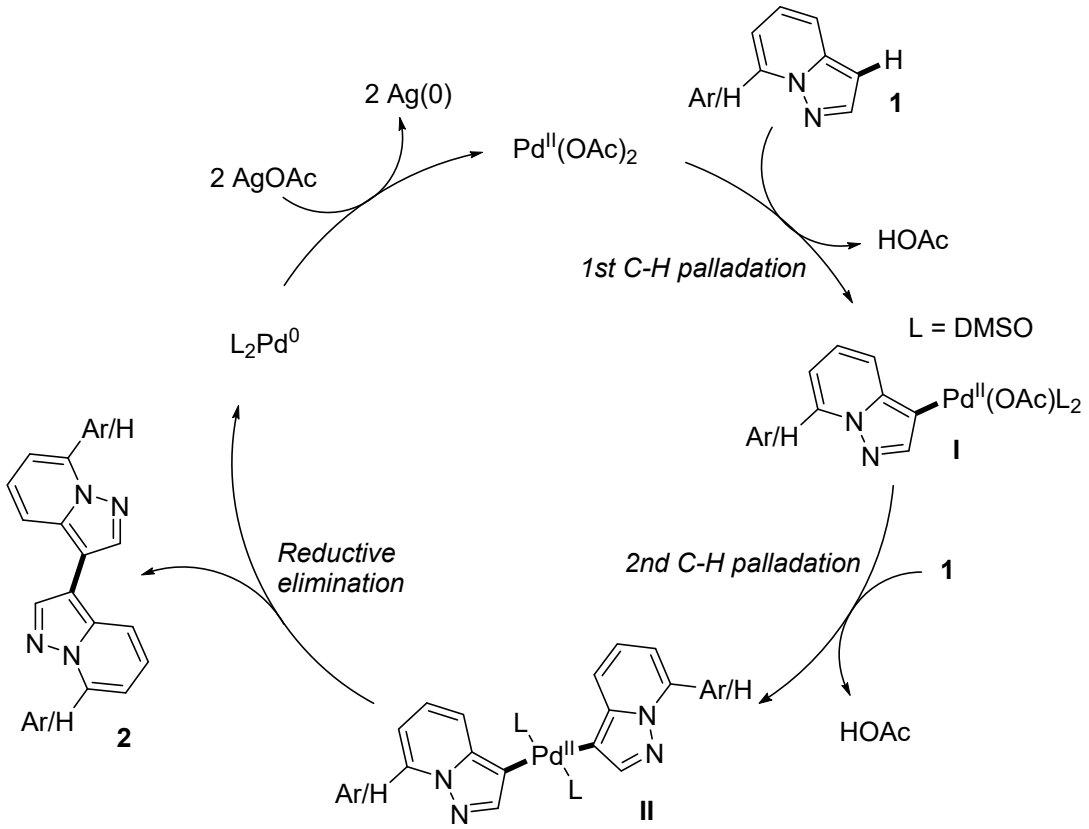

Figure S1. Proposed mechanism for the palladium-catalysed dimerisation of **1** *via* C-H/C-H cross-coupling reaction.

The single crystals of compounds **2a** and **2c** were all grown from the dichloromethane and chloroform solutions by crystallisation at room temperature. Details for the data collection and structure refinement are summarised in Table S1-2. CCDC-2110592 (**2a**) and CCDC-2110591 (**2c**) contain the supplementary crystallographic data for this paper.

Table S1. Crystal data and structure refinement for **2a**.

Empirical formula	$C_{14}H_{10}N_4$	
Formula weight	234.26	
Temperature	200(2) K	
Wavelength	0.71073 Å	
Crystal system	Monoclinic	
Space group	$P\,2_1/n$	
Unit cell dimensions	a = 8.0435(5) Å	α= 90°.
	b = 5.7350(3) Å	β= 99.757(2)°.
	c = 11.9792(8) Å	γ = 90°.
Volume	544.60(6) $Å^3$	
Z	2	
Density (calculated)	1.429 mg/m^3	
Absorption coefficient	0.090 mm^{-1}	
F(000)	244	
Crystal size	0.47 × 0.36 × 0.07 mm^3	
Theta range for data collection	2.84 to 25.48°.	
Index ranges	-9<=h<=9, -6<=k<=6, -14<=l<=14	
Reflections collected	10474	
Independent reflections	988 [R(int) = 0.0533]	
Completeness to theta = 25.48°	98.2 %	
Absorption correction	multi-scan	
Max. and min. transmission	0.9937 and 0.9588	
Refinement method	Full-matrix least-squares on F^2	
Data / restraints / parameters	988 / 0 / 82	
Goodness-of-fit on F^2	1.078	
Final R indices [I>2sigma(I)]	R1 = 0.0327, wR2 = 0.0815	
R indices (all data)	R1 = 0.0398, wR2 = 0.0897	
Largest diff. peak and hole	0.143 and -0.154 $e.Å^{-3}$	

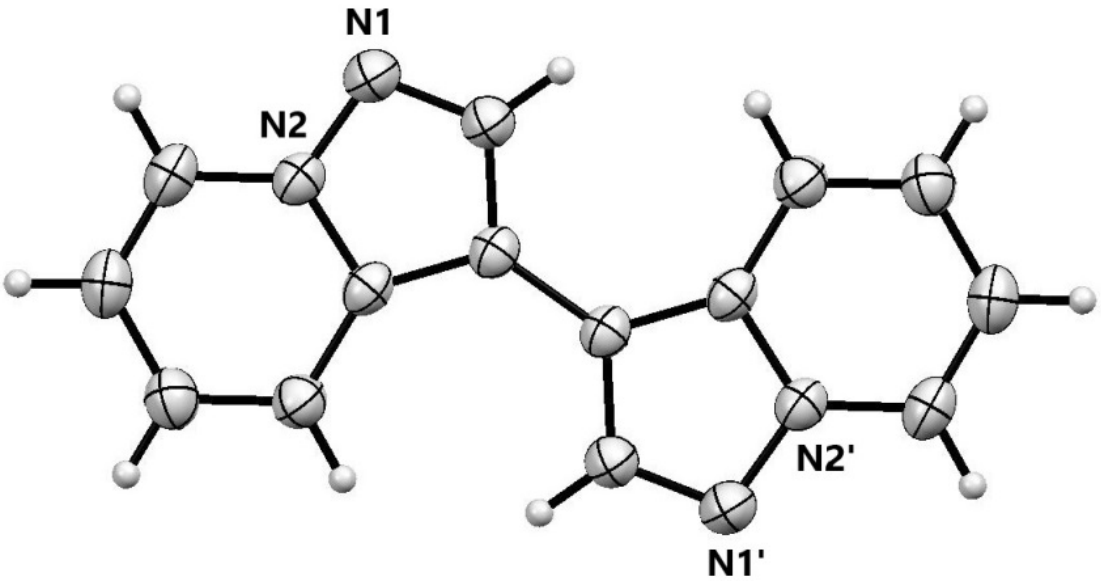

ORTEP diagram of 3,3'-bipyrazolo[1,5-*a*]pyridine (**2a**) with 50% ellipsoidal probability.

Table S2. Crystal data and structure refinement for **2c**.

Empirical formula	$C_{28}H_{22}N_4$	
Formula weight	414.50	
Temperature	200(2) K	
Wavelength	0.71073 Å	
Crystal system	Triclinic	
Space group	*P*-1	
Unit cell dimensions	a = 7.3080(4) Å	α= 86.332(2)°.
	b = 7.5944(4) Å	β= 77.996(2)°.
	c = 9.7428(5) Å	γ = 74.258(2)°.
Volume	509.05(5) $Å^3$	
Z	1	
Density (calculated)	1.352 mg/m^3	
Absorption coefficient	0.081 mm^{-1}	
F(000)	218	
Crystal size	0.47 × 0.31 × 0.06 mm^3	
Theta range for data collection	2.79 to 25.05°.	
Index ranges	-8<=h<=8, -9<=k<=9, -11<=l<=11	
Reflections collected	12502	
Independent reflections	1788 [R(int) = 0.0719]	
Completeness to theta = 25.05°	99.2 %	
Absorption correction	multi-scan	
Max. and min. transmission	0.9951 and 0.9628	
Refinement method	Full-matrix least-squares on F^2	
Data / restraints / parameters	1788 / 0 / 146	
Goodness-of-fit on F^2	1.063	
Final R indices [I>2sigma(I)]	R1 = 0.0395, wR2 = 0.0943	
R indices (all data)	R1 = 0.0555, wR2 = 0.1068	
Largest diff. peak and hole	0.194 and -0.196 $e.Å^{-3}$	

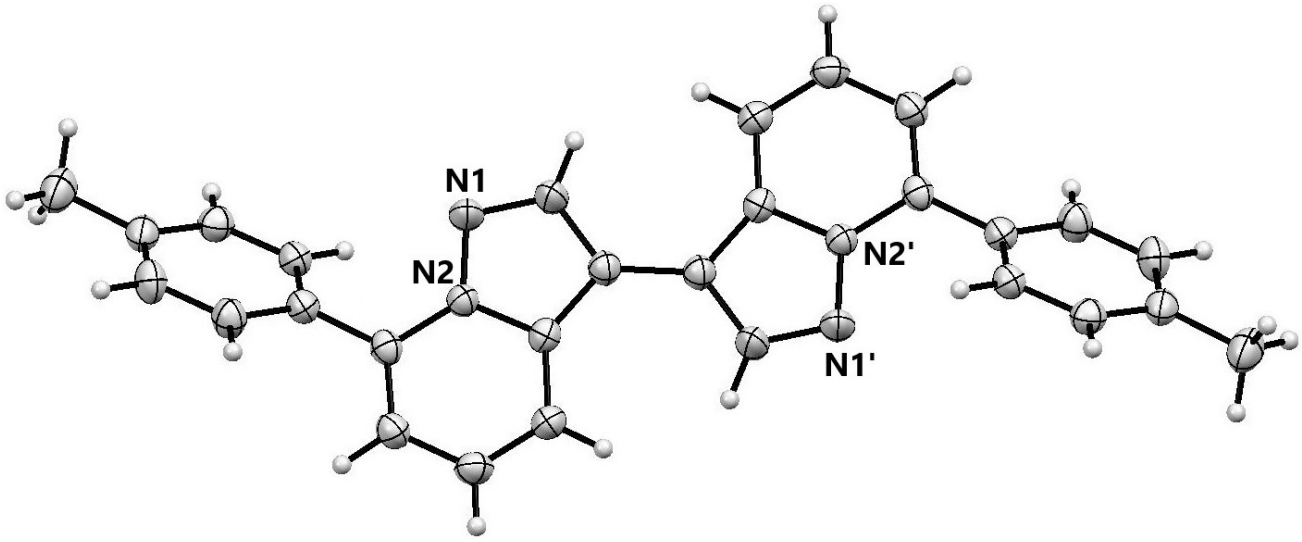

ORTEP diagram of 7,7'-di-*p*-tolyl-3,3'-bipyrazolo[1,5-*a*]pyridine (**2c**) with 50% ellipsoidal probability.

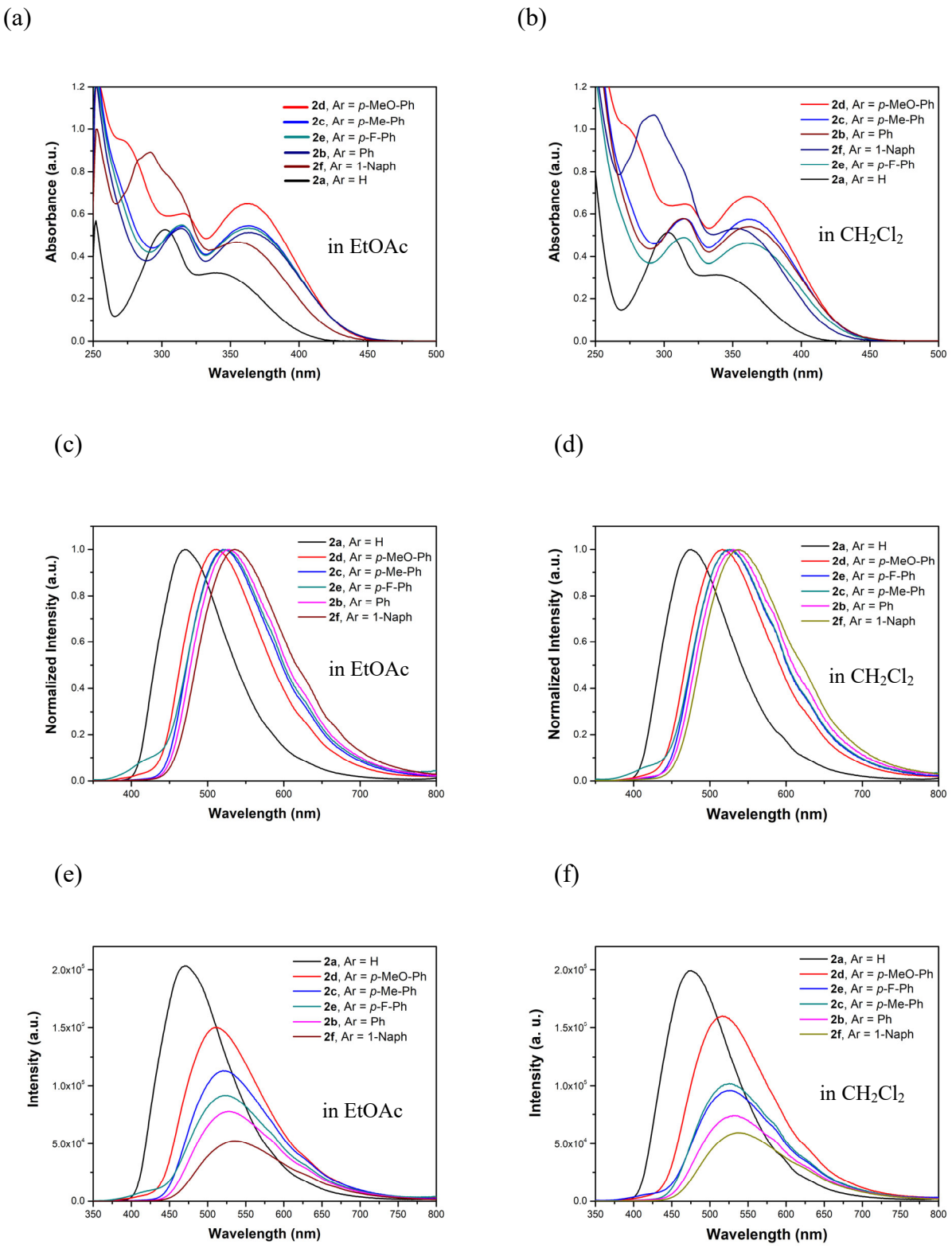

Figure S2. (a-b) Absorption spectra (5.0 x 10^{-5} M), (c-d) Normalised fluorescence spectra, and (e-f) Fluorescence spectra of **2a-f** in ethyl acetate solutions (1.0 x 10^{-4} M, λ_{ex} = 295 nm for **2a-c**, **2e-f** and 335 nm for **2d**) and dichloromethane solutions (1.0 x 10^{-4} M, λ_{ex} = 303 nm for **2a**; 295 nm for **2b,d-e**; 315 nm for **2c**; and 310 nm for **2f**), respectively.

Table S3. Photophysical properties of **2a-f**.

Entry	Compound	λ_{abs} (nm)	ε_{max} ($M^{-1}cm^{-1}$)	λ_{fl} (nm)	Stokes shift (nm)	Φ_{fl}
1	**2a**[a]	302, 340	11000, 7000	471	131	0.2[c]
2	**2a**[b]	303, 338	10200, 6200	476	138	0.22[d]
3	**2b**[a]	314, 366	11000, 11000	526	160	0.09[c]
4	**2b**[b]	314, 359	11500, 10800	530	171	0.08[d]
5	**2c**[a]	315, 363	12000, 12000	522	159	0.10[c]
6	**2c**[b]	315, 361	11600, 11600	526	165	0.11[d]
7	**2d**[a]	316, 363	13000, 14000	513	150	0.18[c]
8	**2d**[b]	315, 361	13100, 13800	516	155	0.17[d]
9	**2e**[a]	315, 364	12000, 11000	526	162	0.10[c]
10	**2e**[b]	315, 361	9800, 9300	526	165	0.11[d]
11	**2f**[a]	292, 355	19000, 10000	536	181	0.06[c]
12	**2f**[b]	293, 352	21300, 10800	538	186	0.06[d]

[a,b] Absorption (5.0×10^{-5} M) and fluorescence (1.0×10^{-4} M) spectra were recorded in ethyl acetate solutions (λ_{ex} = 295 nm for **2a-c**,**e-f** and 335 nm for **2d**) and dichloromethane solutions (λ_{ex} = 303 nm for **2a**; 295 nm for **2b,d-e**; 315 nm for **2c**; and 310 nm for **2f**), respectively, at room temperature.

[c,d] Quantum yields were measured in 3.5×10^{-6} M of ethyl acetate solutions and 2.5×10^{-6} M of dichloromethane solutions, respectively, at room temperature and the reference standard is 0.1 M H_2SO_4 (aq) of quinine sulfate (λ_{ex} = 340 nm, quantum yield = 0.54).

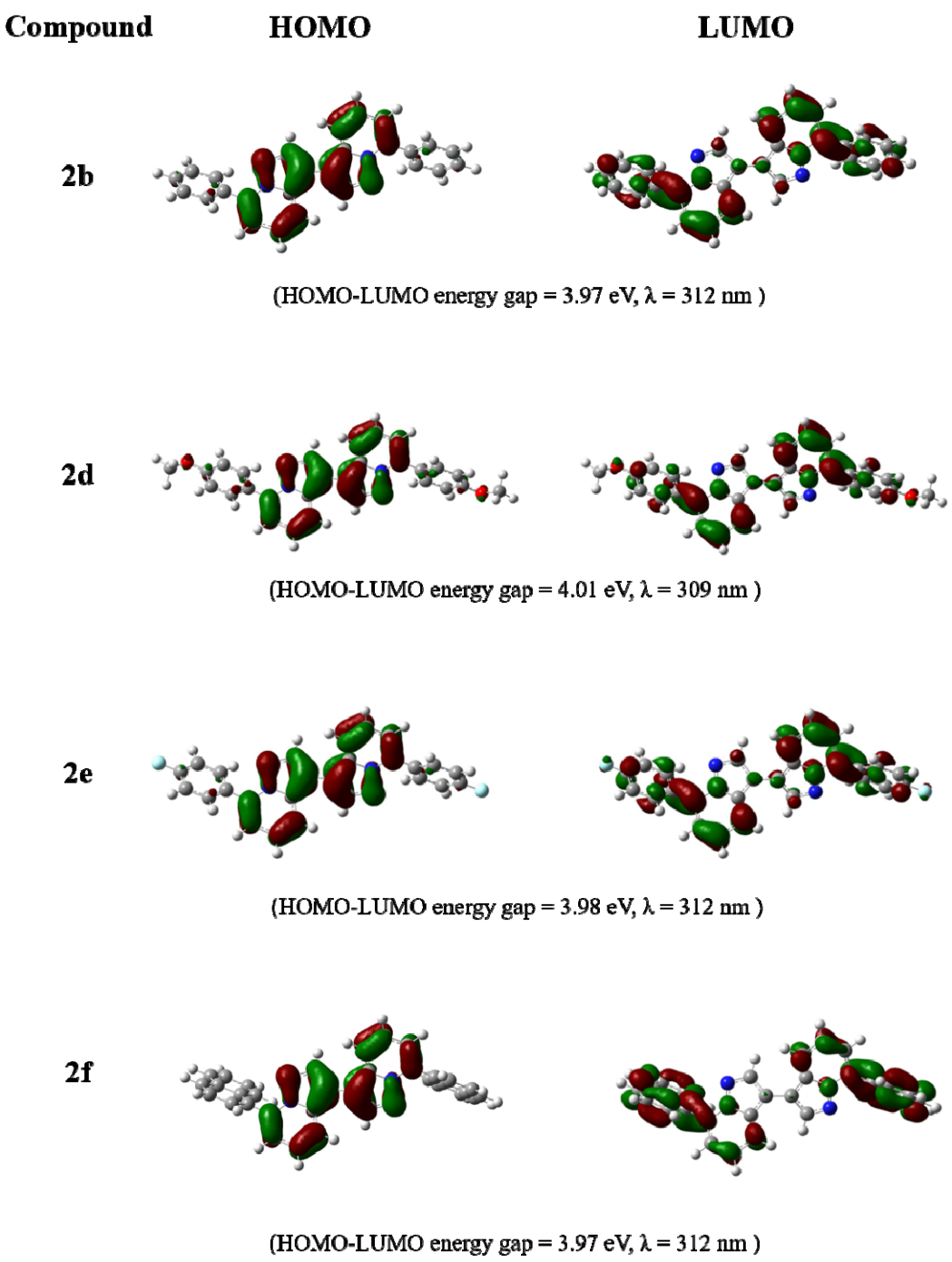

Figure S3. HOMO-LUMO molecular maps of compounds **2b**,**d-f**.

Computational details:

All calculations were performed with Gaussian 09 program package. Geometry optimisations and vibrational frequency calculations were carried out at the B3LYP−D3/6−31G(d) level in the gas phase. On basis of geometries calculated at the B3LYP−D3/6−31G(d) level in the gas phase, the corresponding single−point electronic energies were calculated at M06−D3/6−311++G(d,p) level of theory with an SMD continuum solvation model (dichloromethane). All the discussed energies in this paper refer to solvation electronic energy values.

(I)

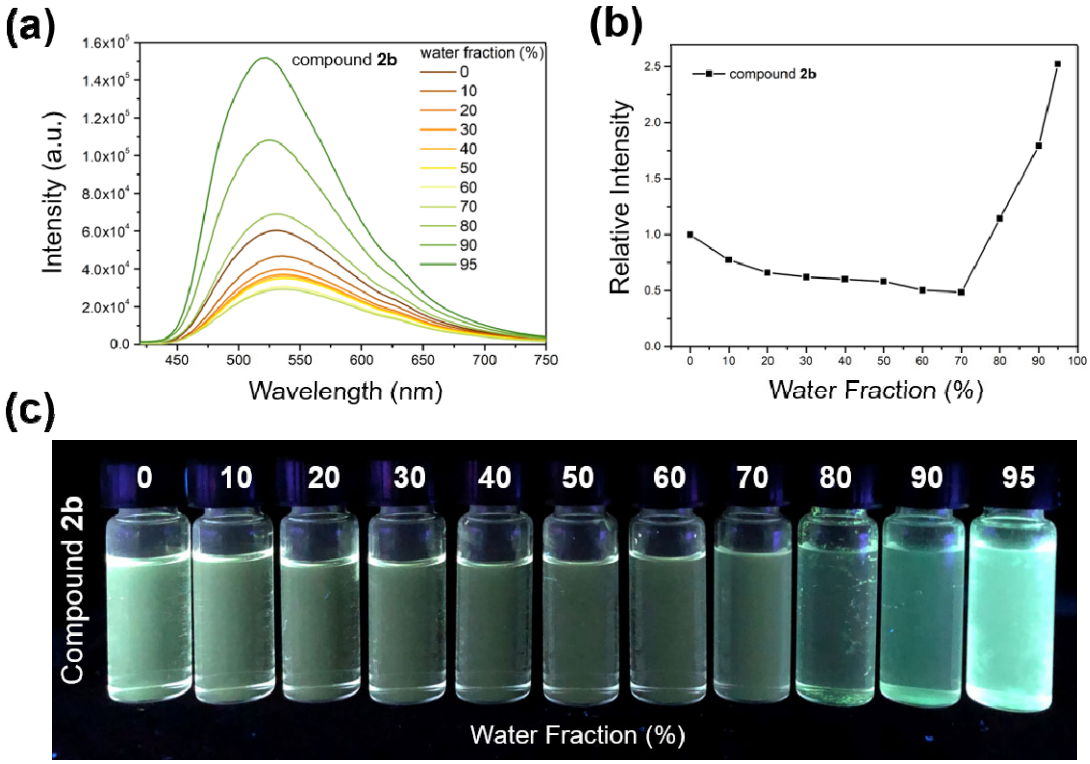

(II)

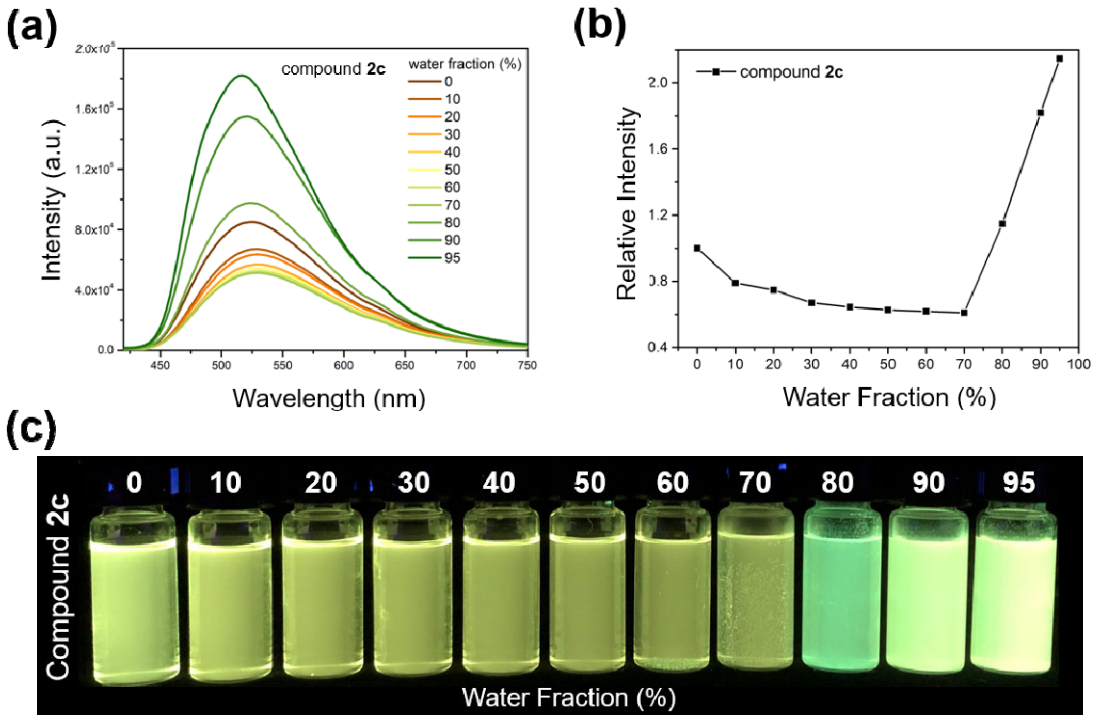

(Continued on the next page)

(III)

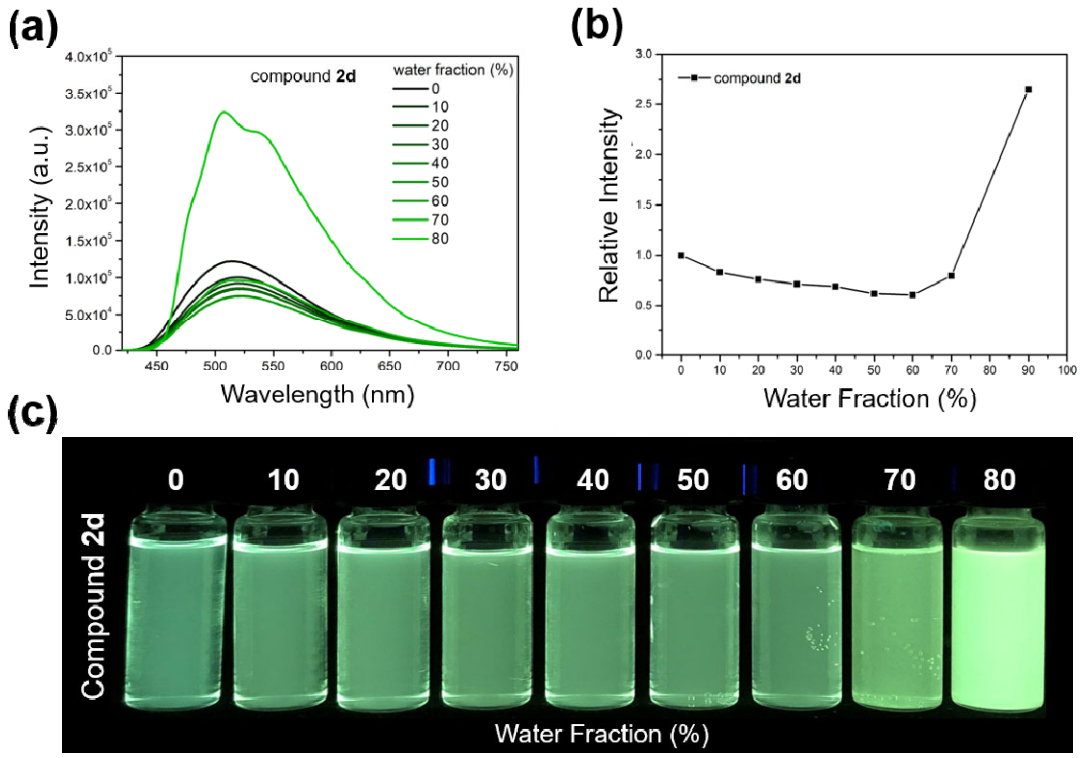

(IV)

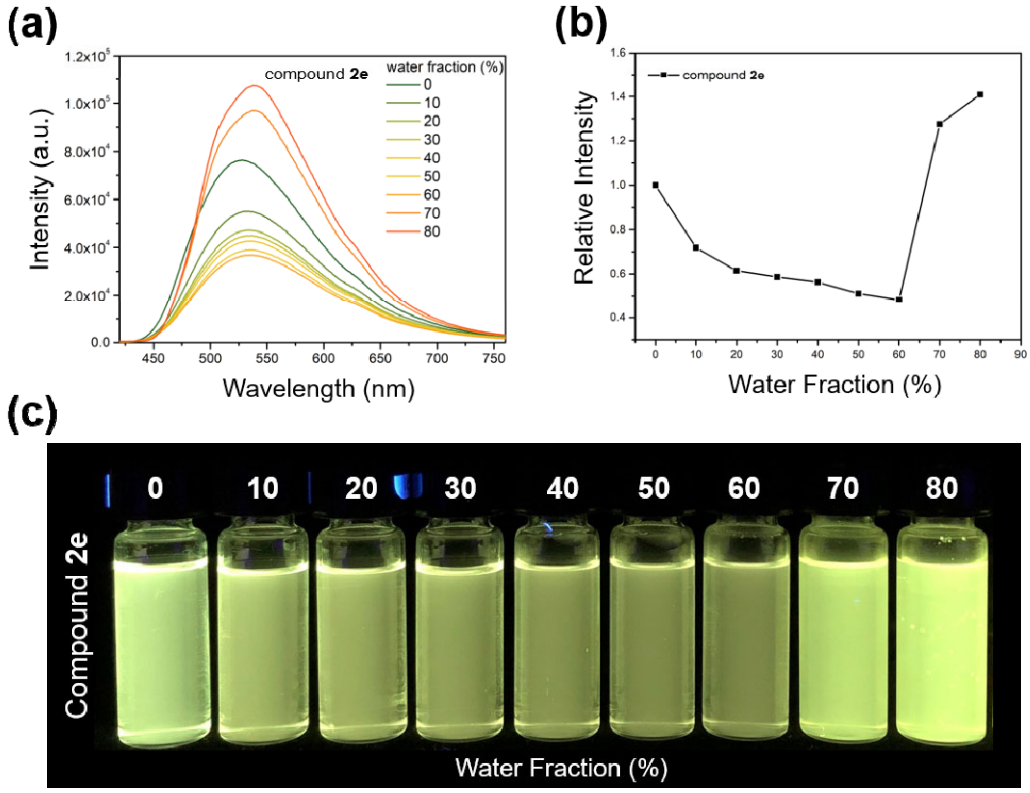

Figure S4. (a) Emission spectra (1.5×10^{-4} M, λ_{ex} = 400 nm), (b) the relative fluorescence intensity vs. water fraction plot, and (c) fluorescence images under UV light (365 nm) of compounds (I) **2b**, (II) **2c**, (III) **2d**, and (IV) **2e** in THF/H_2O mixtures with different water fractions from 0 up to 95%.

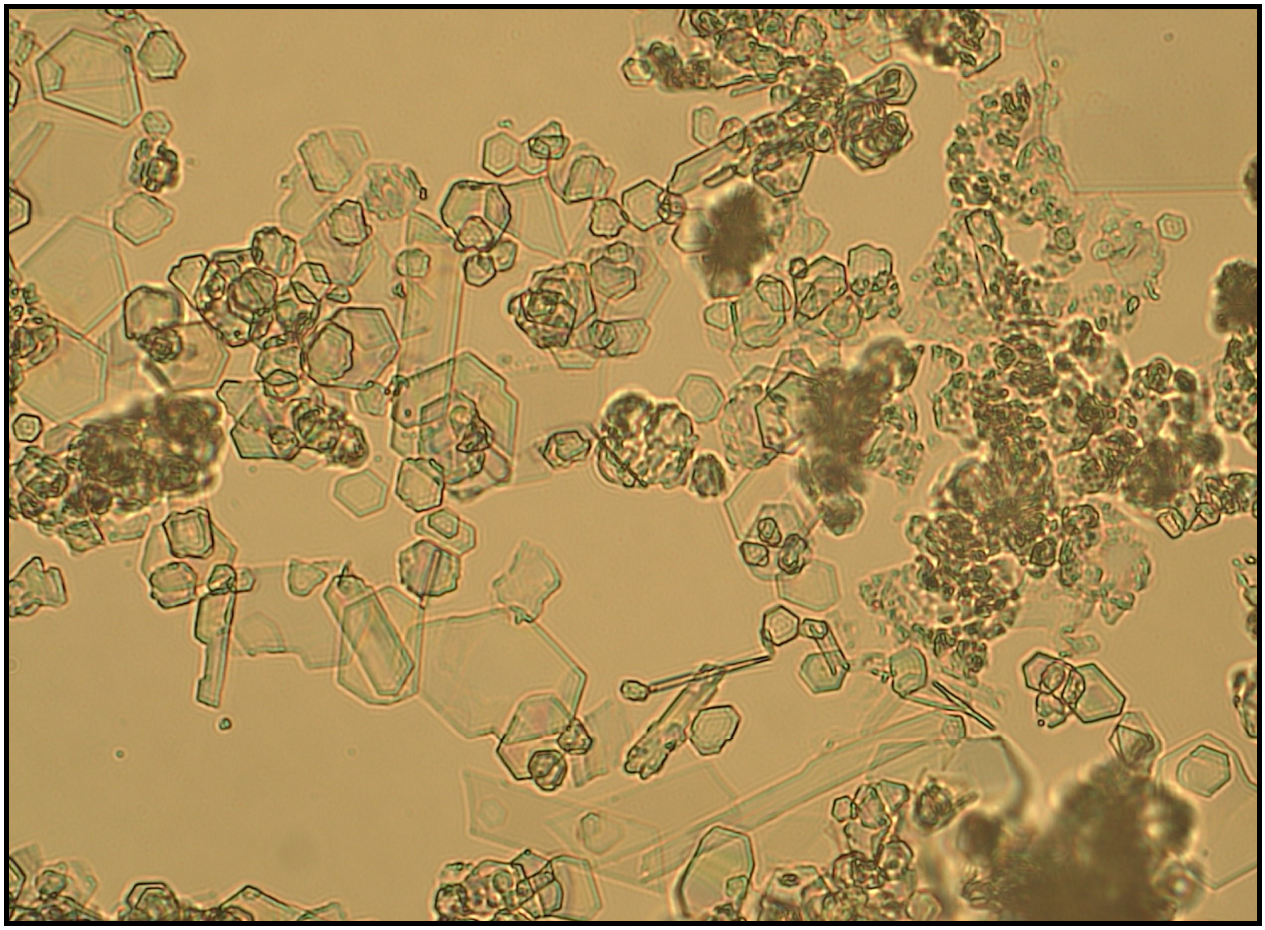

Figure S5. An optical microscopic image (magnified by 60 times) of compound **2f** in the aggregate state.

Table S4. Fluorescence quantum yields (Φ_{fl}) and lifetimes (τ_{fl}) of compound **2f** in THF/H_2O mixtures with 0, 30, 60, 80, and 90% water fractions.

Entry	Water fraction (%)	Φ_{fl}[a]	τ_{fl} (ns)
1	0	0.05[b]	1.11
2	30	0.05	0.85
3	60	0.03	1.21
4	80	0.07	2.96
5	90	0.33	3.15

[a] Quantum yields were measured in 3.8×10^{-6} M of THF/H_2O solutions at room temperature and the reference standard is 0.1 M H_2SO_4 (aq) of quinine sulfate (λ_{ex} = 340 nm, quantum yield = 0.54). [b] The quantum yield was measured in 7.5×10^{-6} M of THF solution.

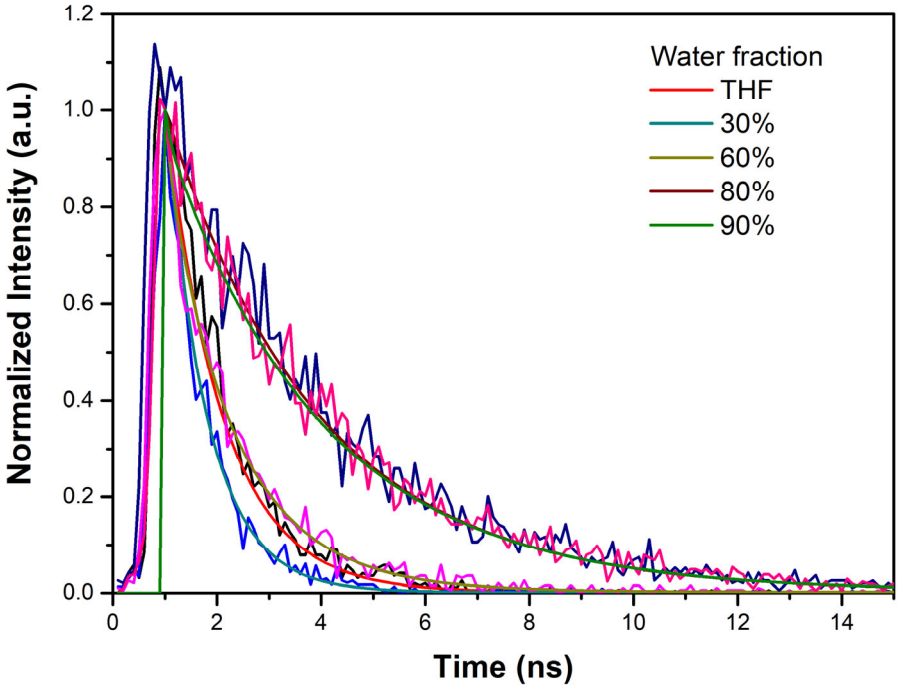

Figure S6. Fluorescence lifetime measurements of compound **2f** in THF/H_2O mixtures with 0, 30, 60, 80, and 90% water fractions.

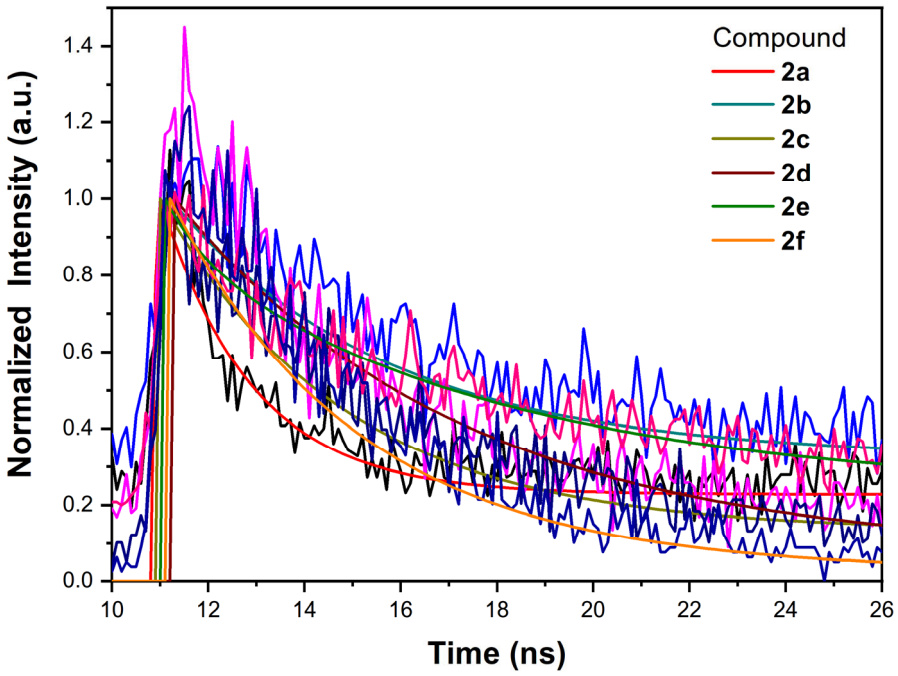

Figure S7. Fluorescence lifetime measurements of compounds **2a-f** in the solid-state.

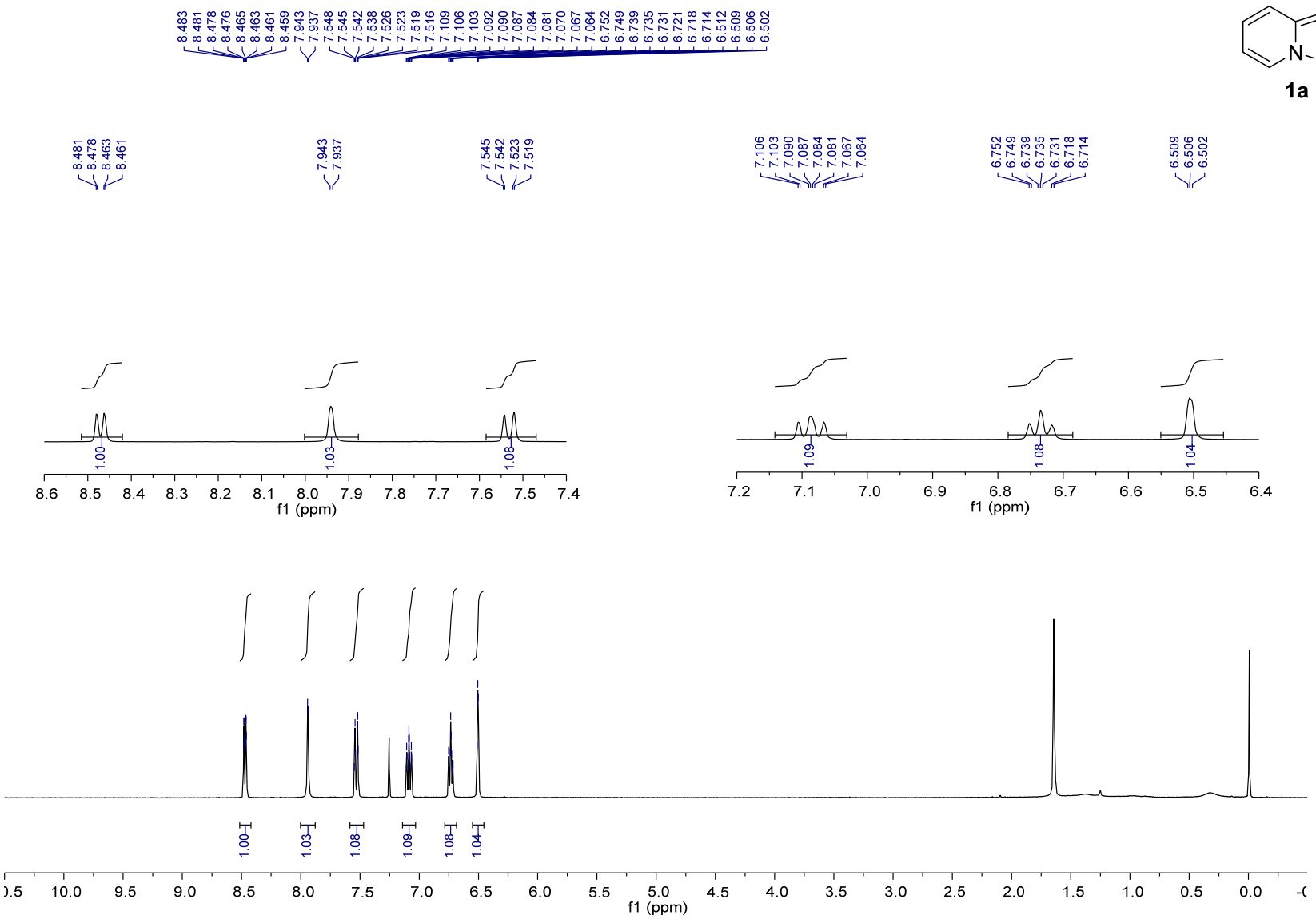

Figure S8. ^{1}H NMR spectrum of **1a** (400 MHz, $CDCl_3$).

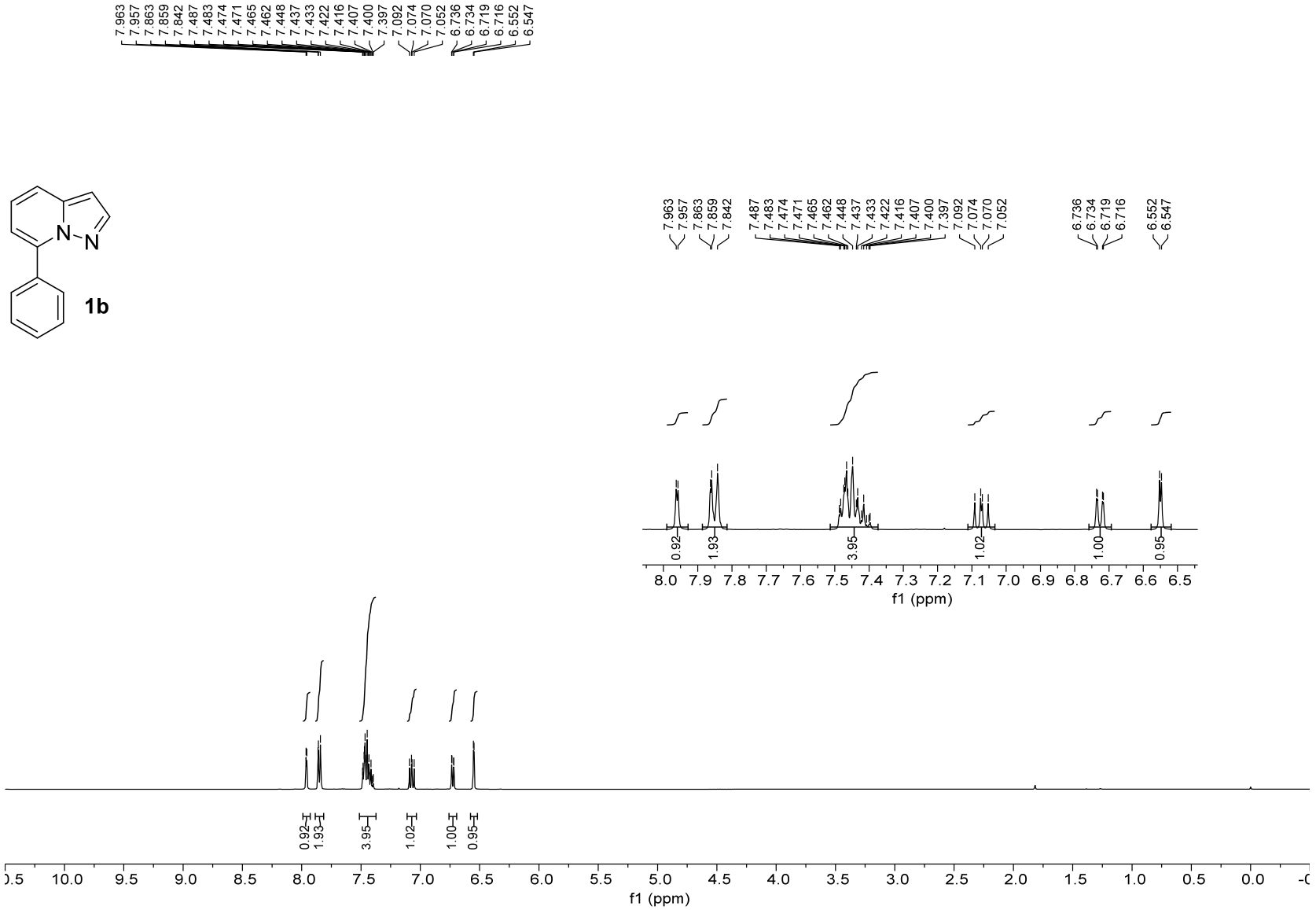

Figure S9. ^{1}H NMR spectrum of **1b** (400 MHz, $CDCl_3$).

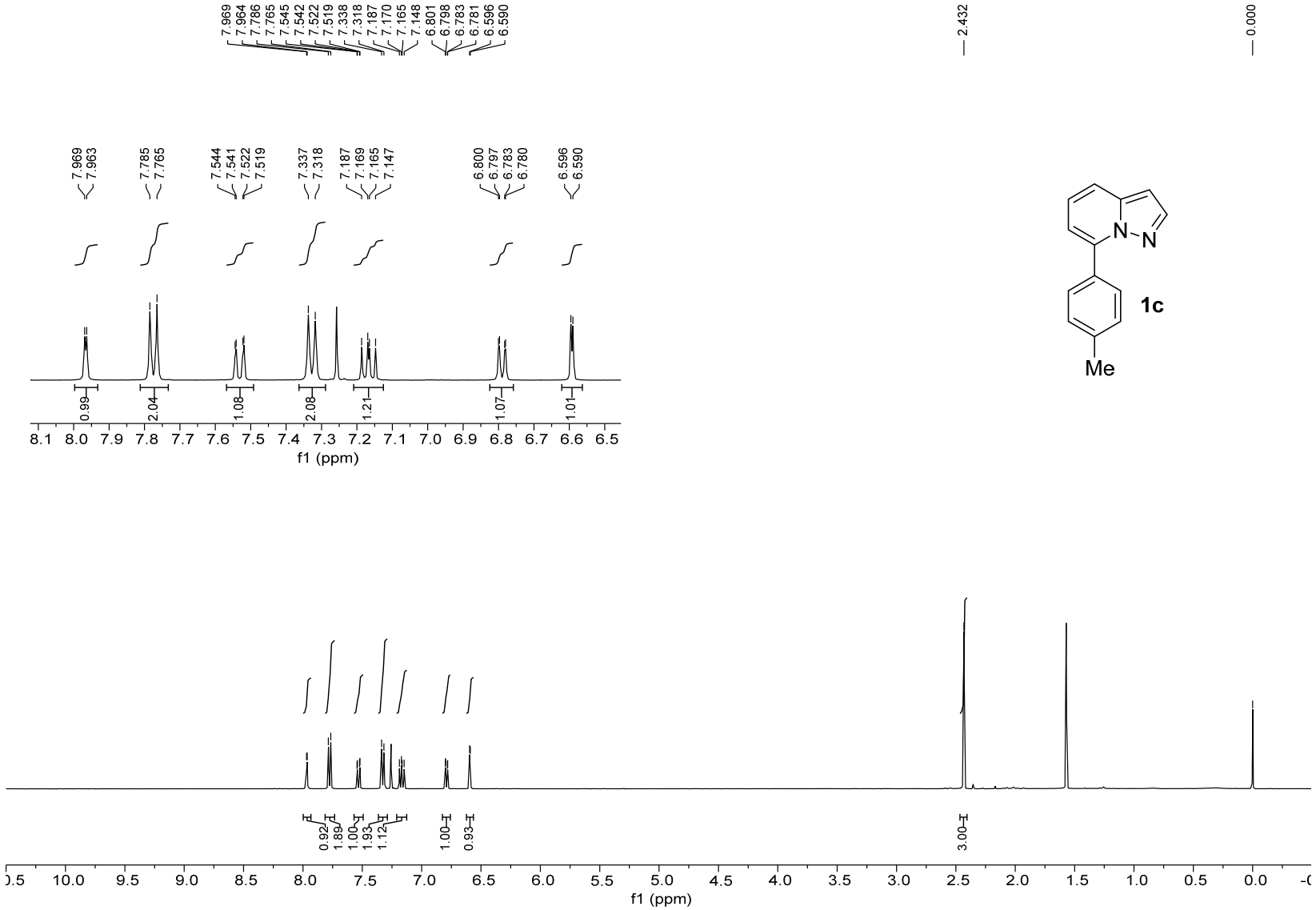

Figure S10. ^{1}H NMR spectrum of **1c** (400 MHz, $CDCl_3$).

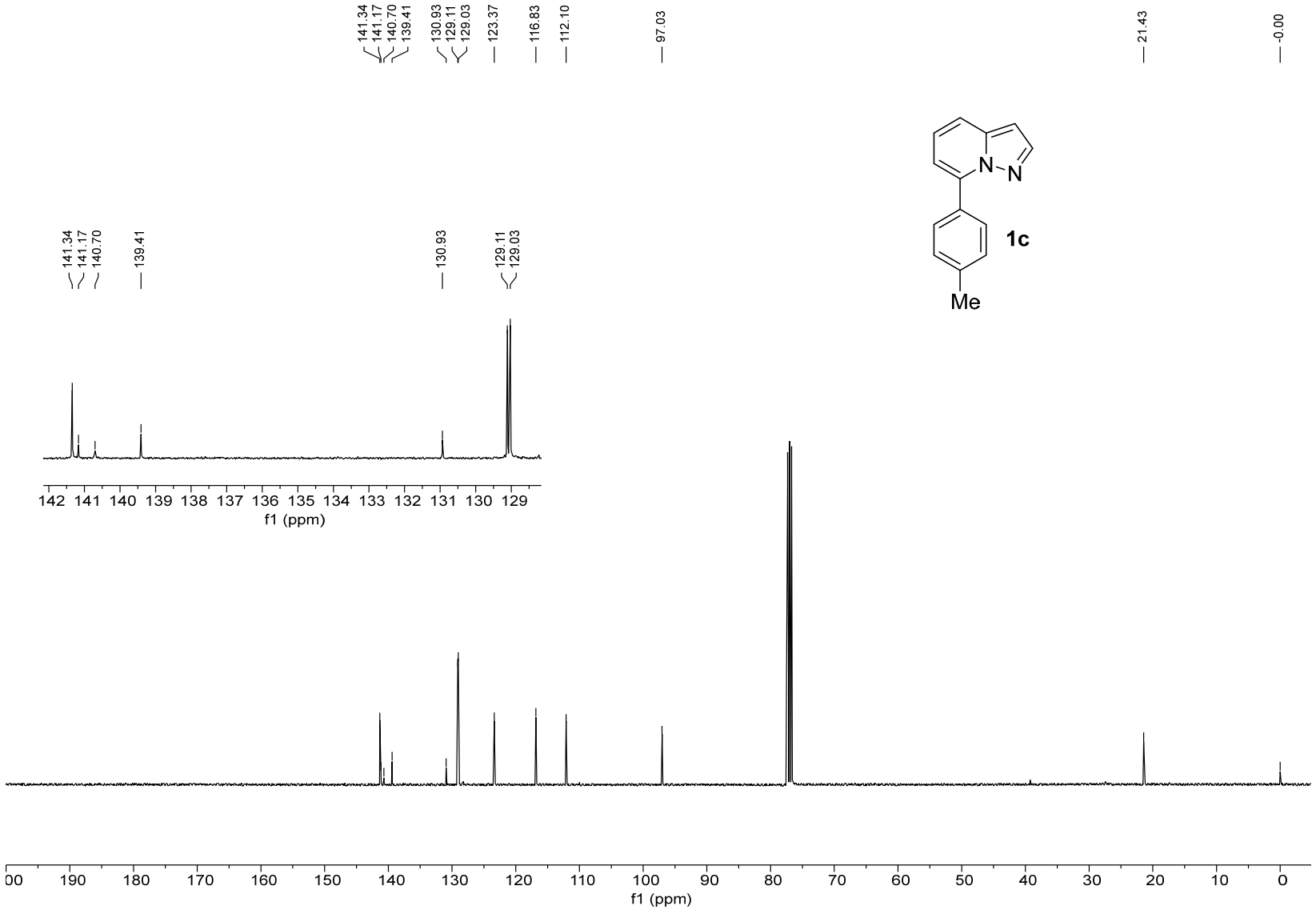

Figure S11. ^{13}C NMR spectrum of **1c** (101 MHz, $CDCl_3$).

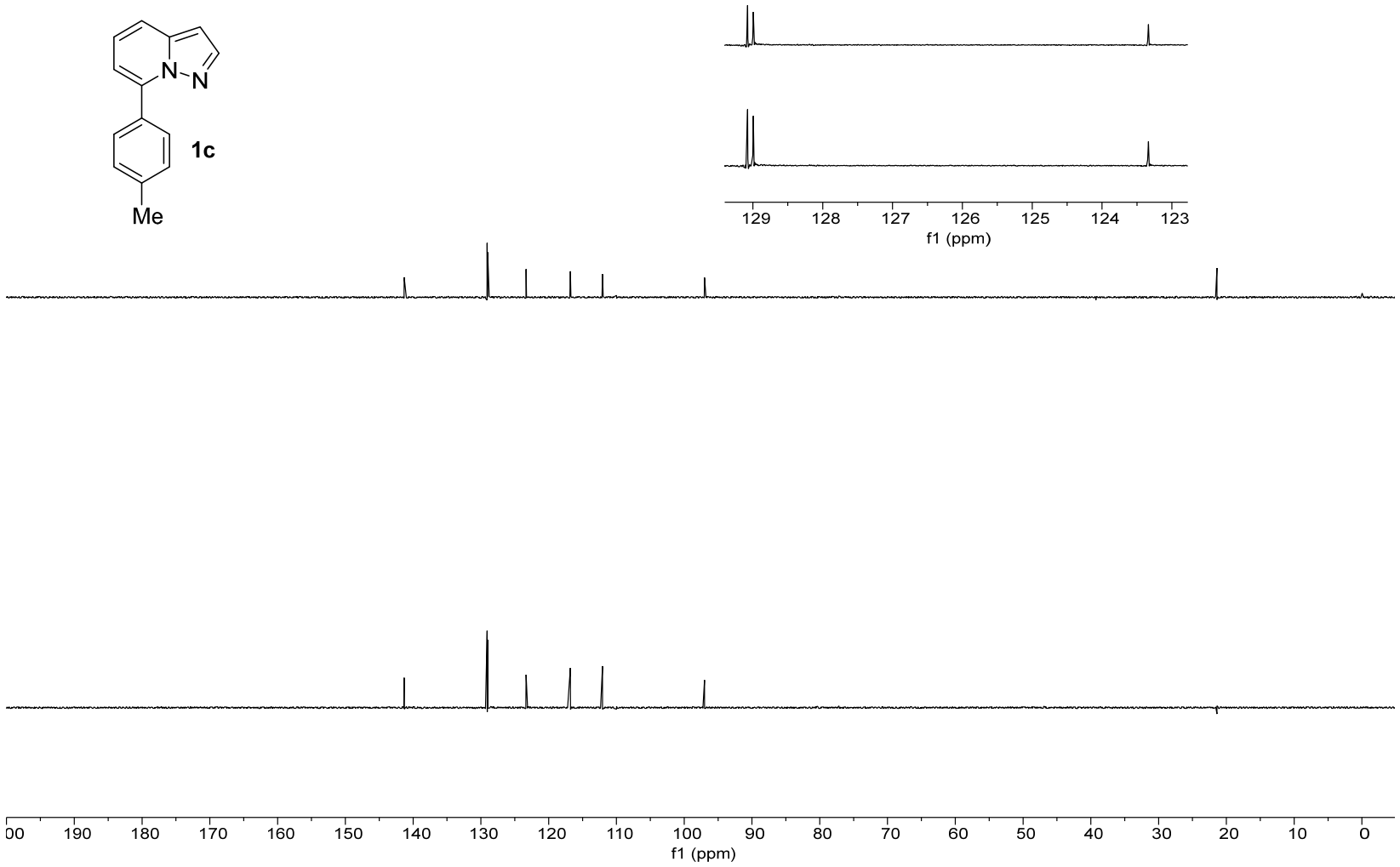

Figure S12. DEPT (90 and 135°) NMR spectra of **1c** (101 MHz, $CDCl_3$).

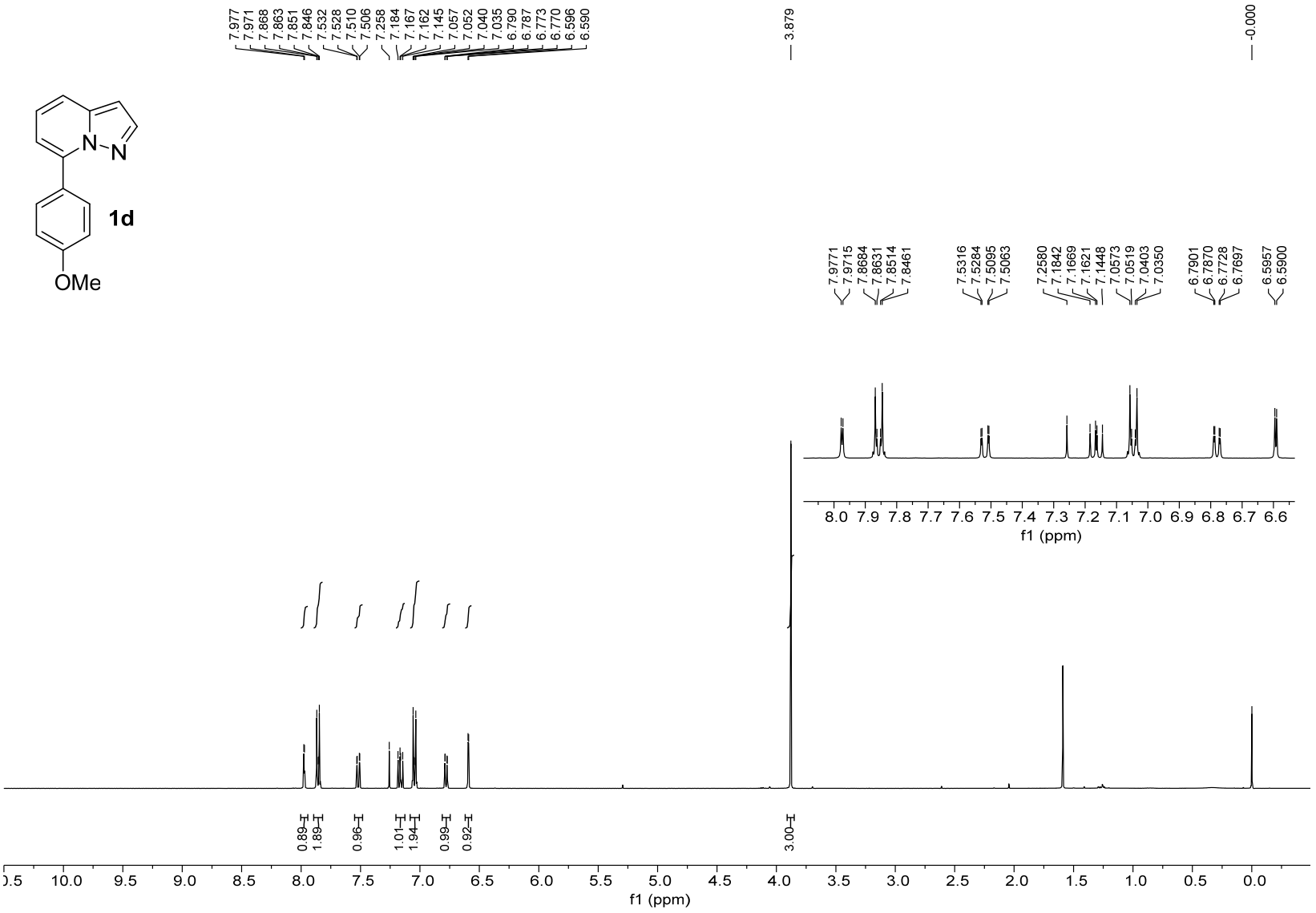

Figure S13. ^{1}H NMR spectrum of **1d** (400 MHz, $CDCl_3$).

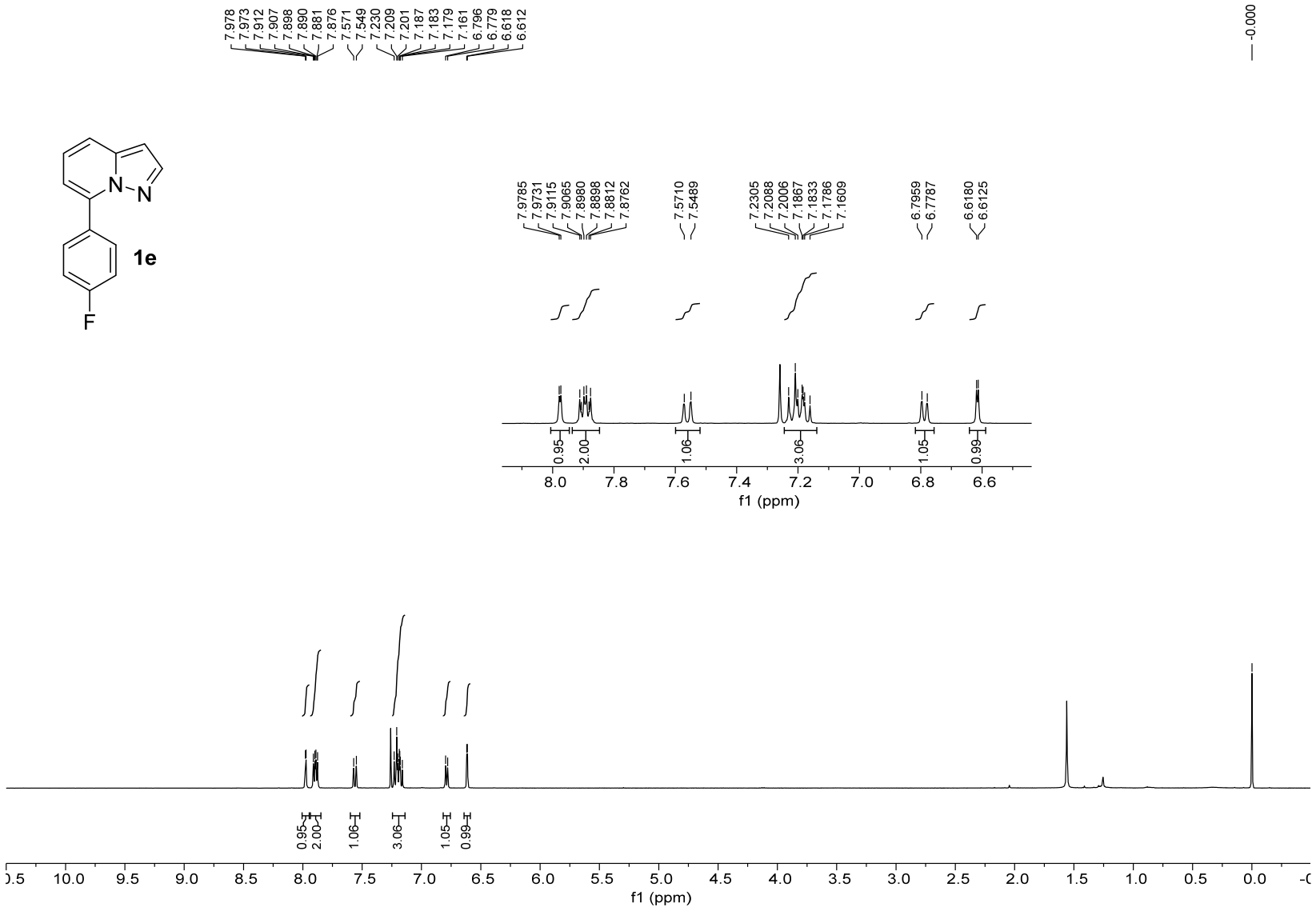

Figure S14. ^{1}H NMR spectrum of **1e** (400 MHz, $CDCl_3$).

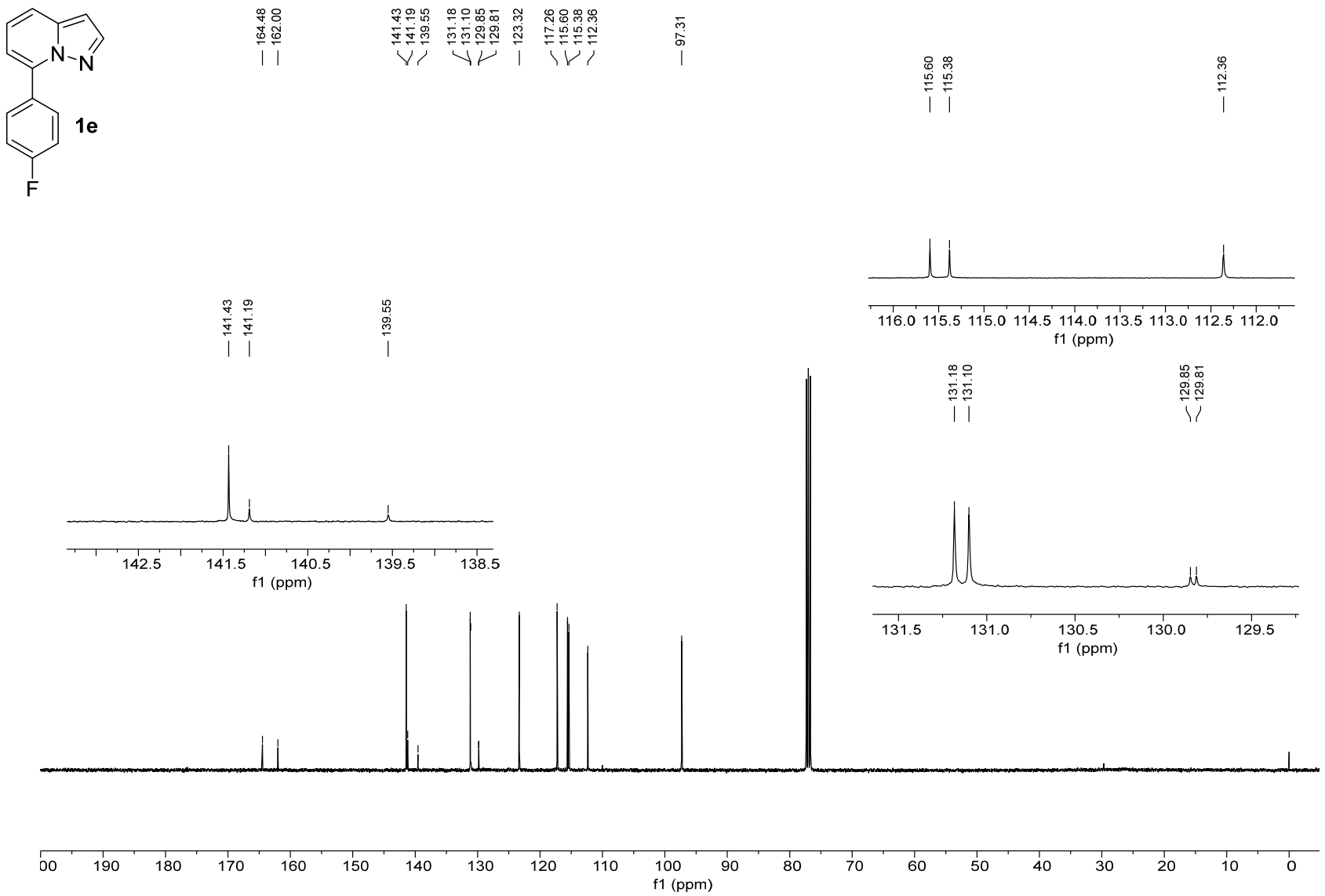

Figure S15. ^{13}C NMR spectrum of **1e** (101 MHz, $CDCl_3$).

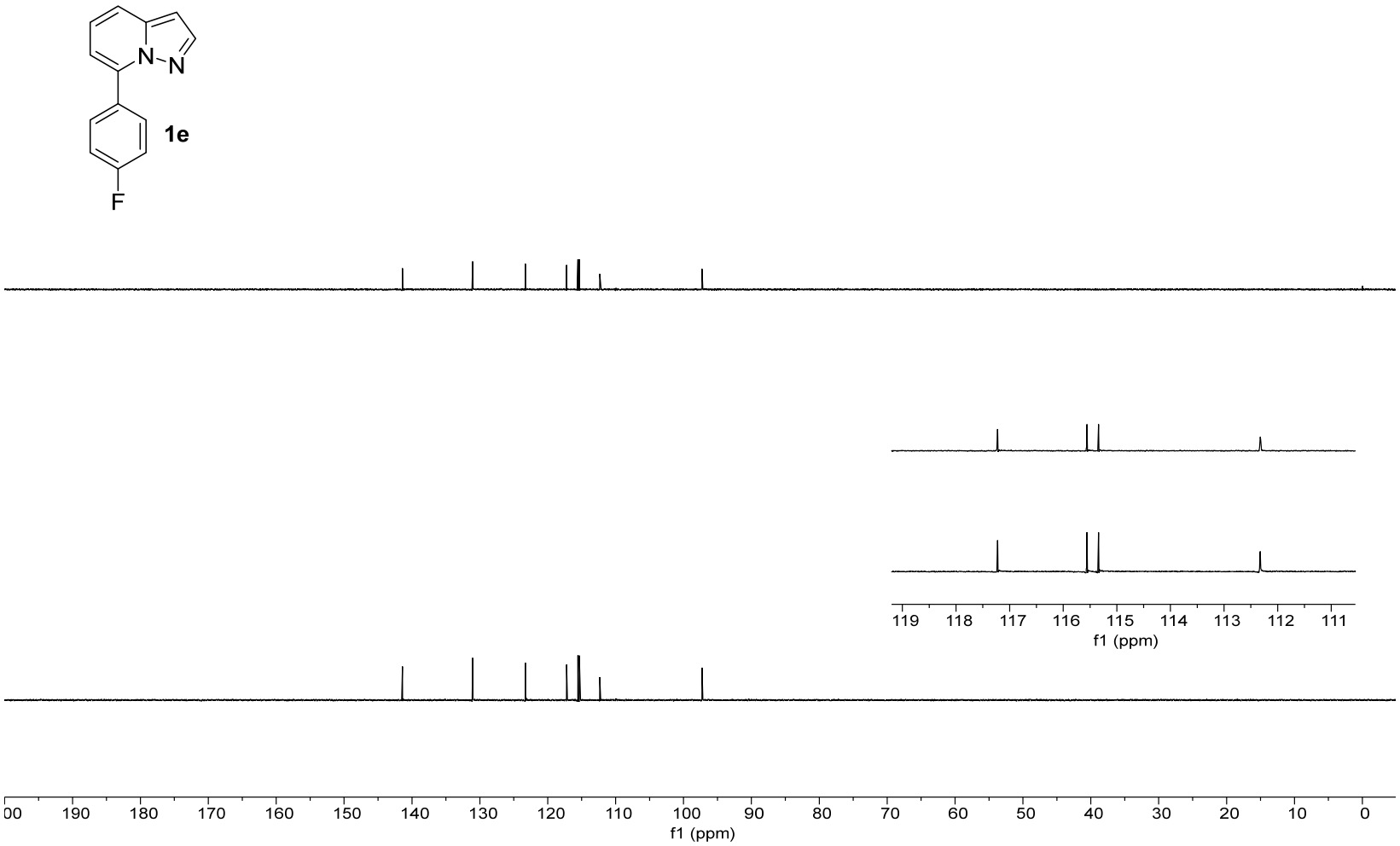

Figure S16. DEPT (90 and 135º) NMR spectra of **1e** (101 MHz, $CDCl_3$).

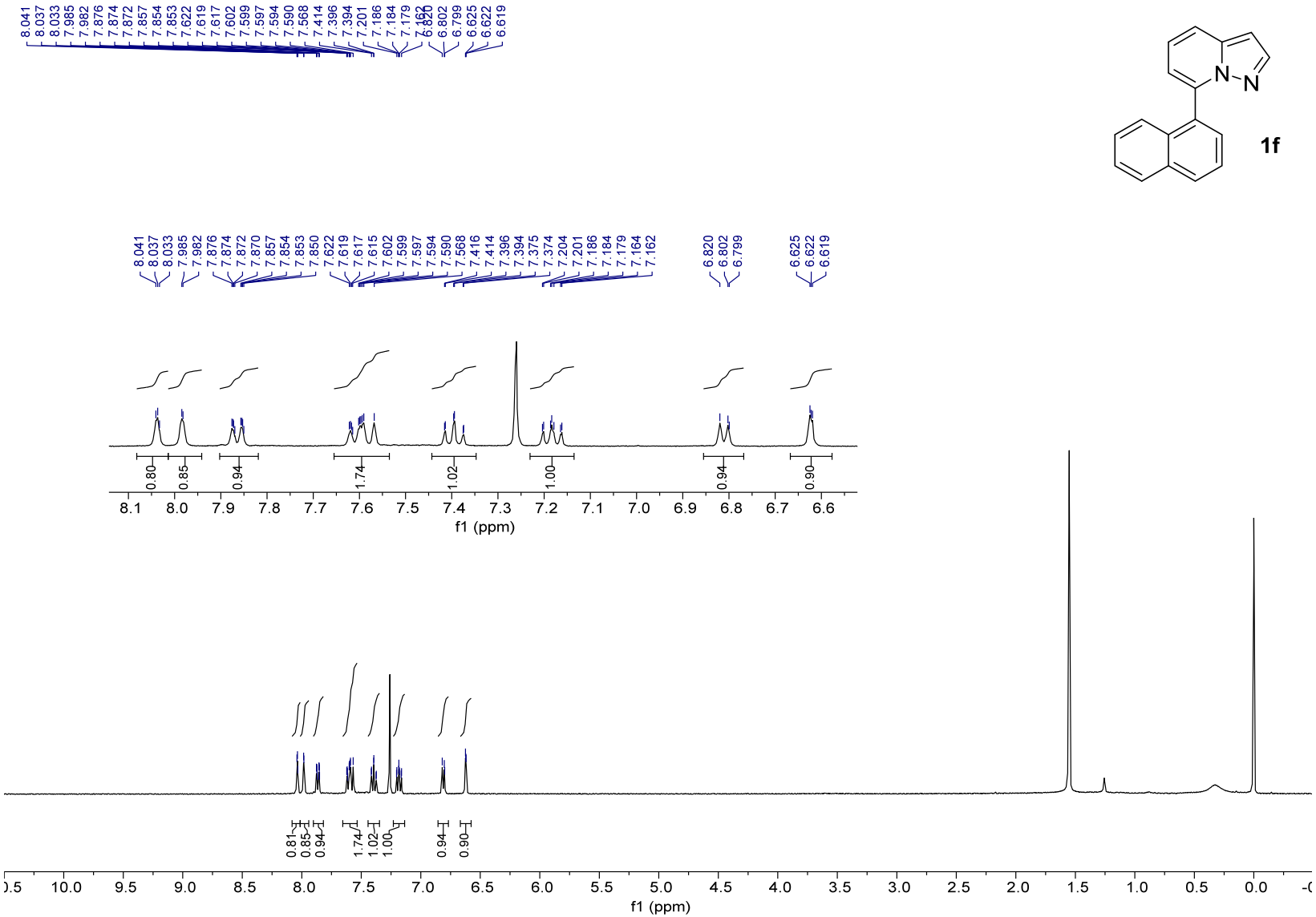

Figure S17. ^{1}H NMR spectrum of **1f** (400 MHz, $CDCl_3$).

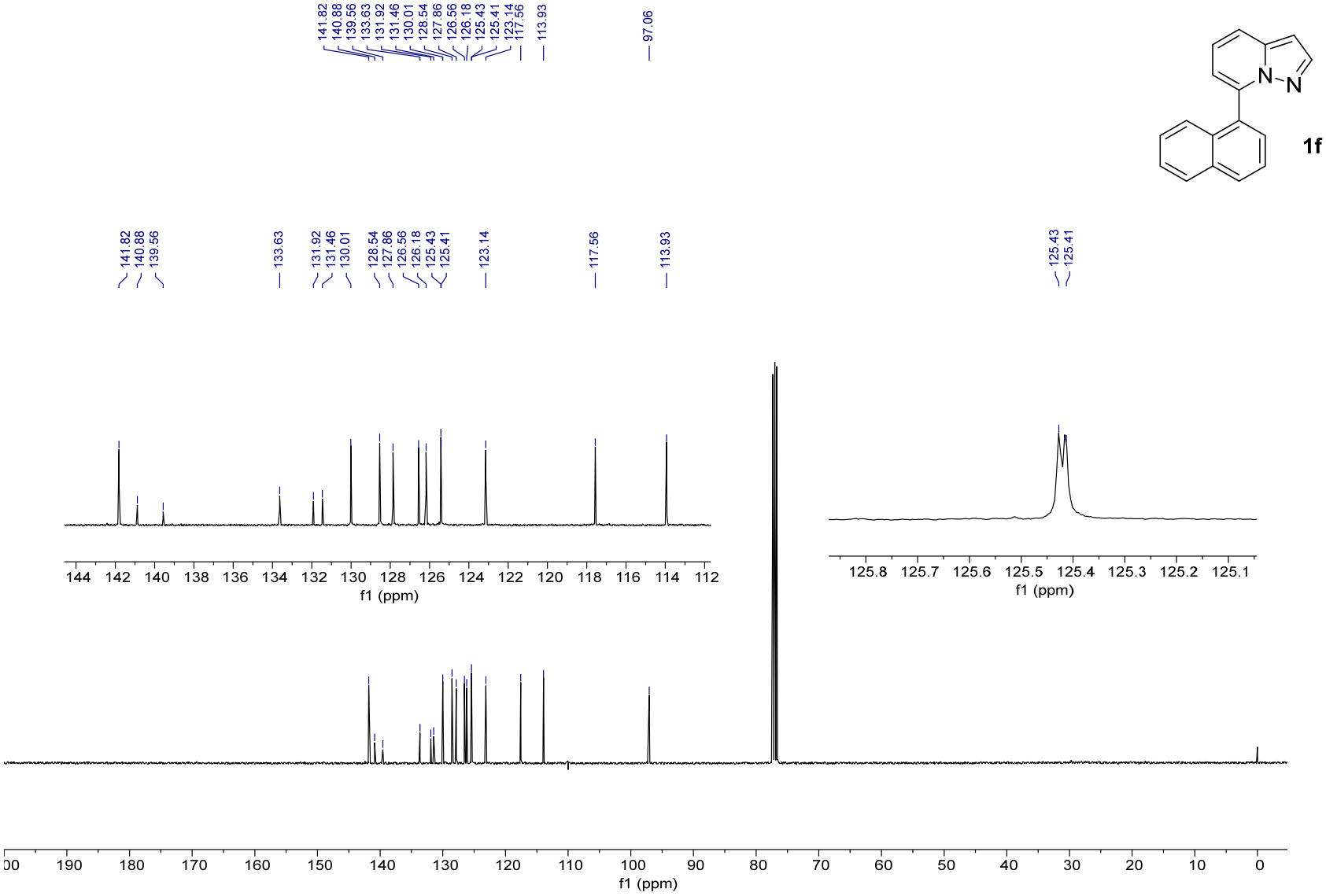

Figure S18. ^{13}C NMR spectrum of **1f** (101 MHz, $CDCl_3$).

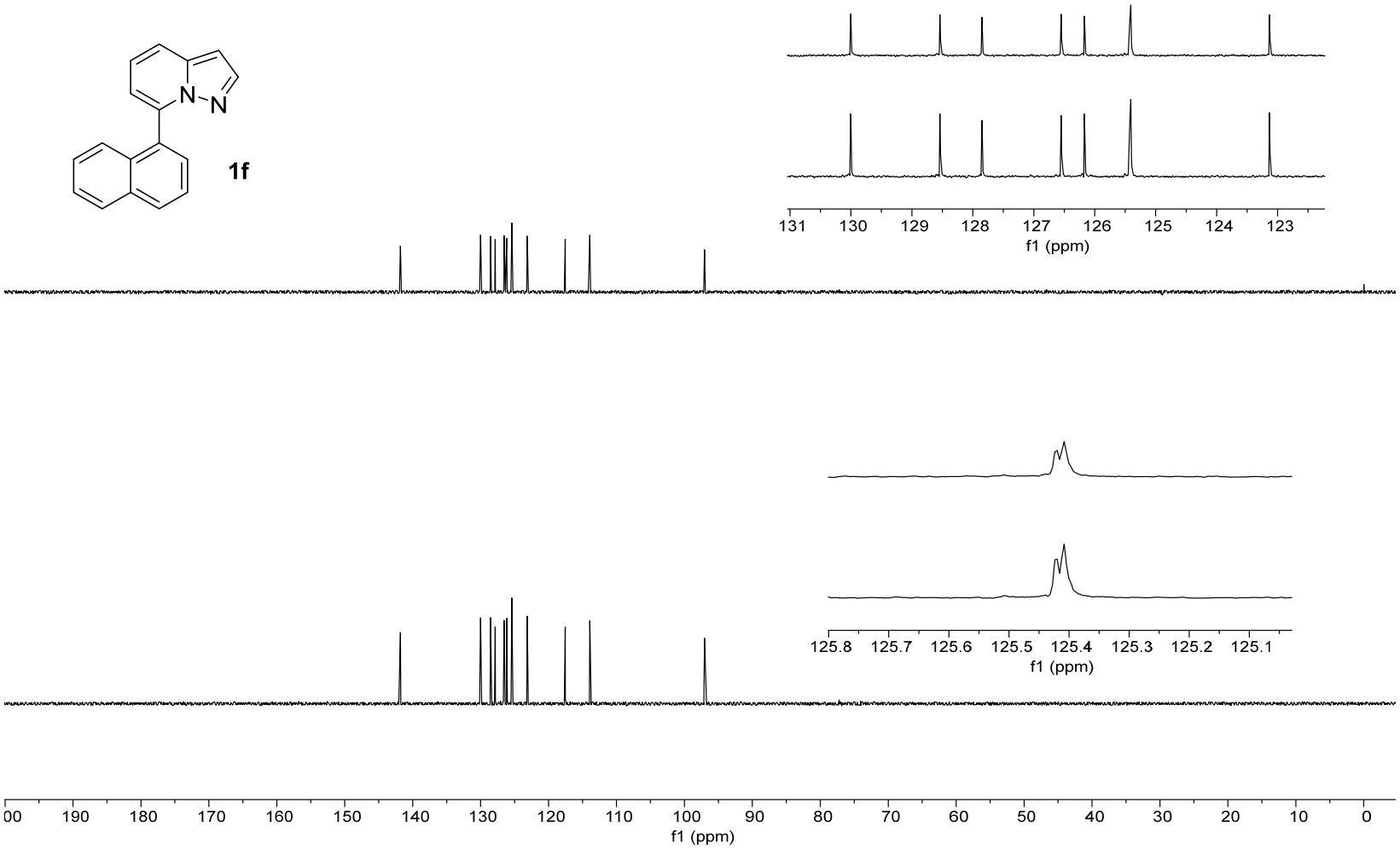

Figure S19. DEPT (90 and 135º) NMR spectra of **1f** (101 MHz, $CDCl_3$).

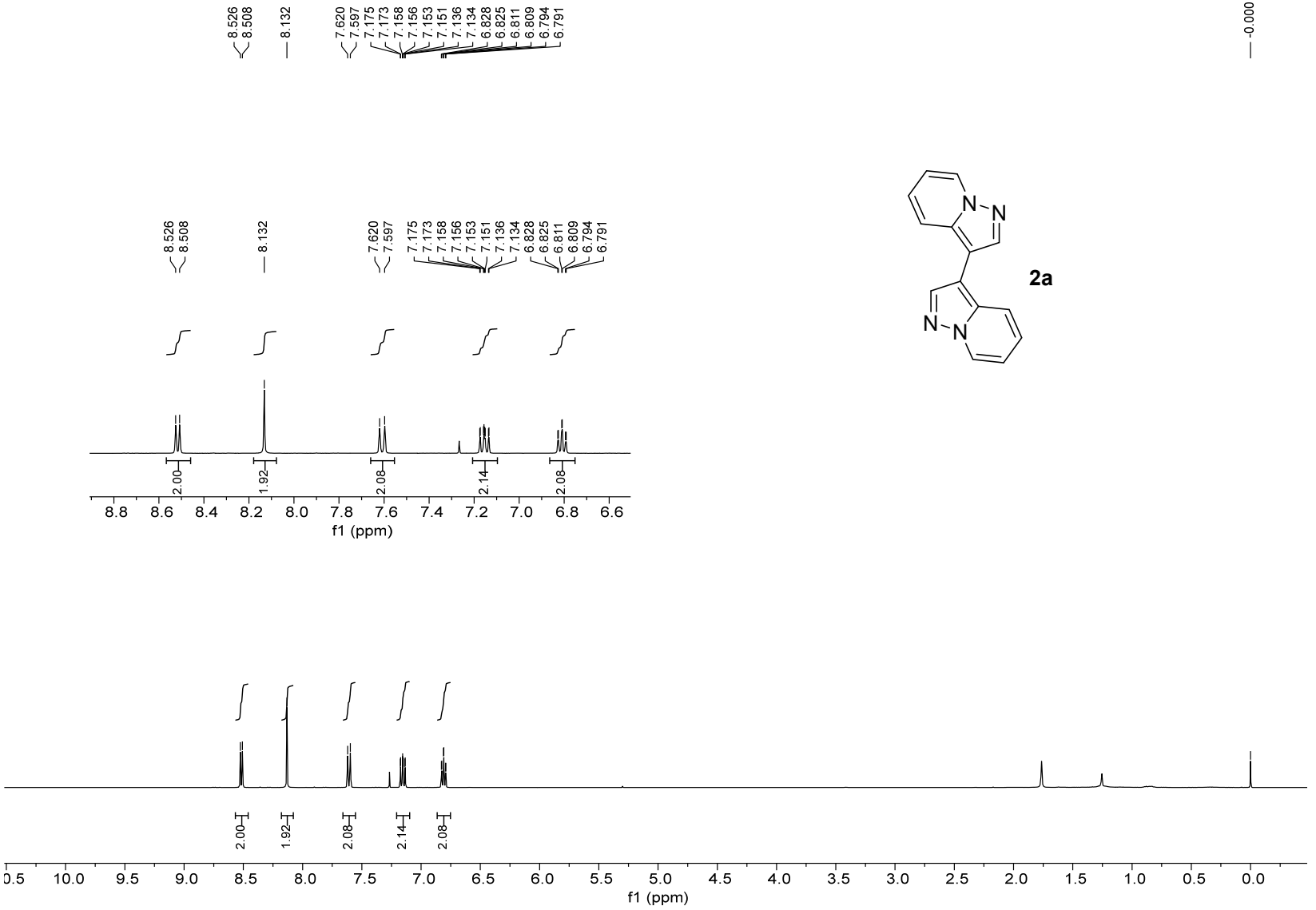

Figure S20. ^{1}H NMR spectrum of **2a** (400 MHz, $CDCl_3$).

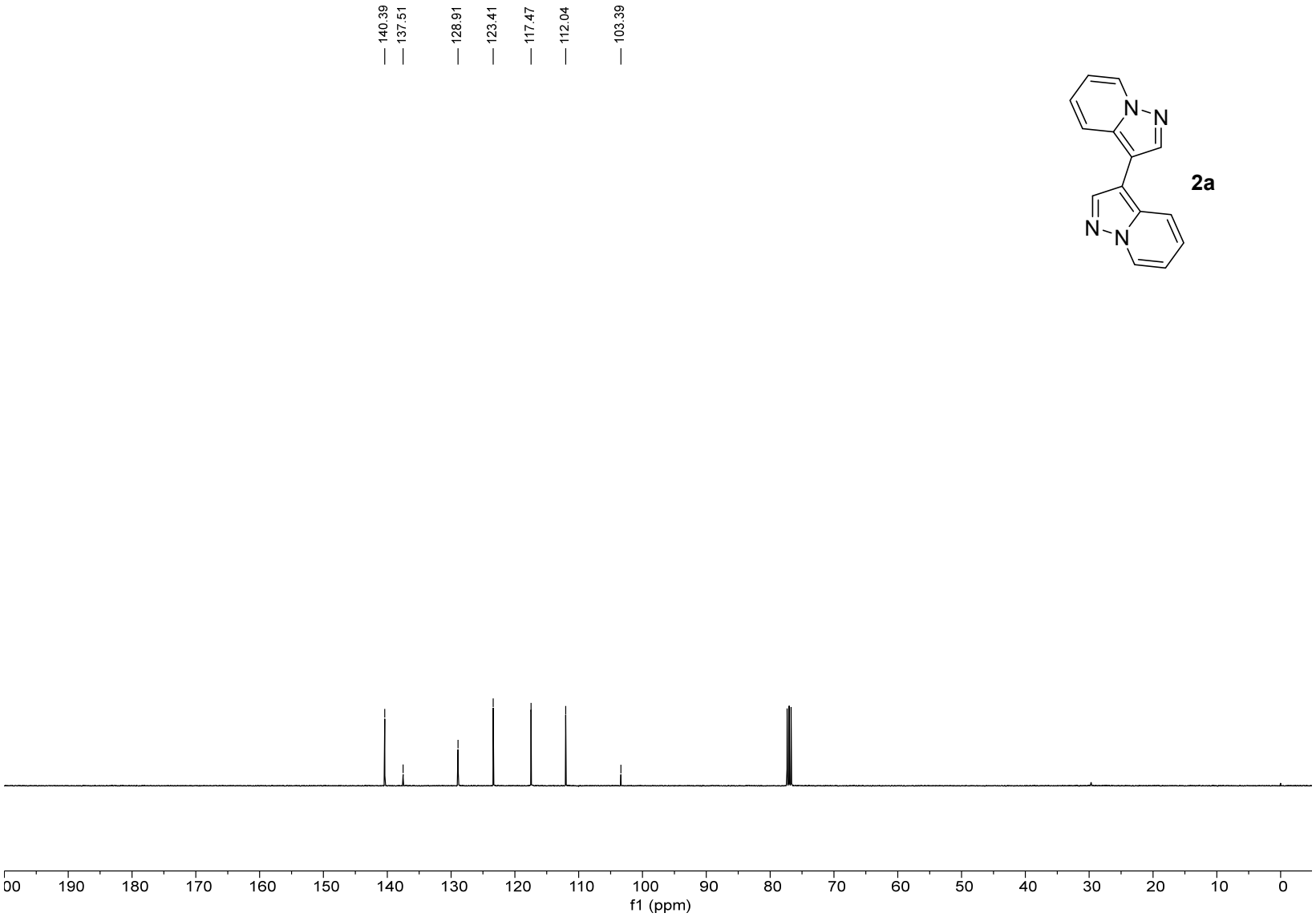

Figure S21. ^{13}C NMR spectrum of **2a** (101 MHz, $CDCl_3$).

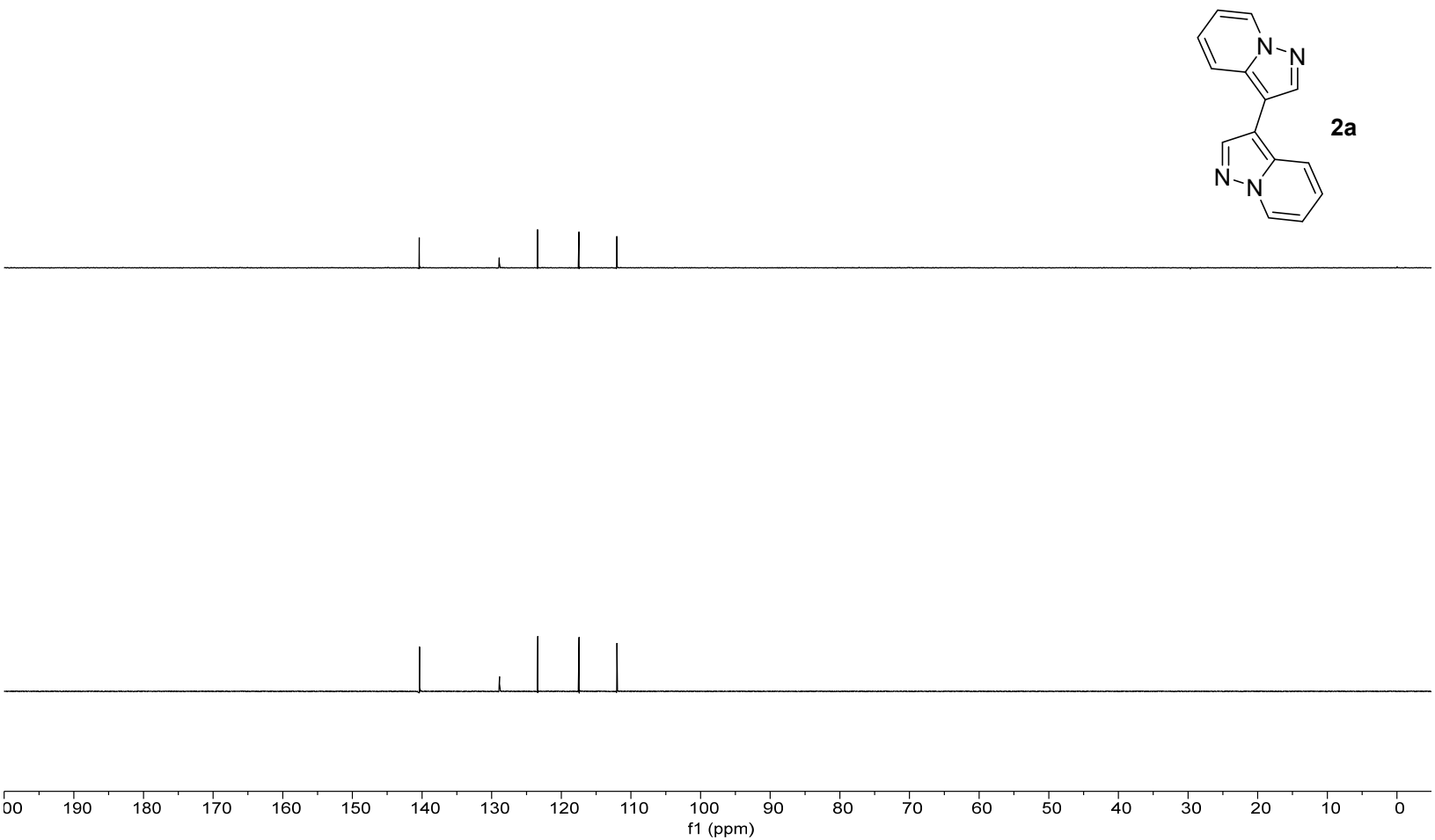

Figure S22. DEPT (90 and 135º) NMR spectra of **2a** (101 MHz, $CDCl_3$).

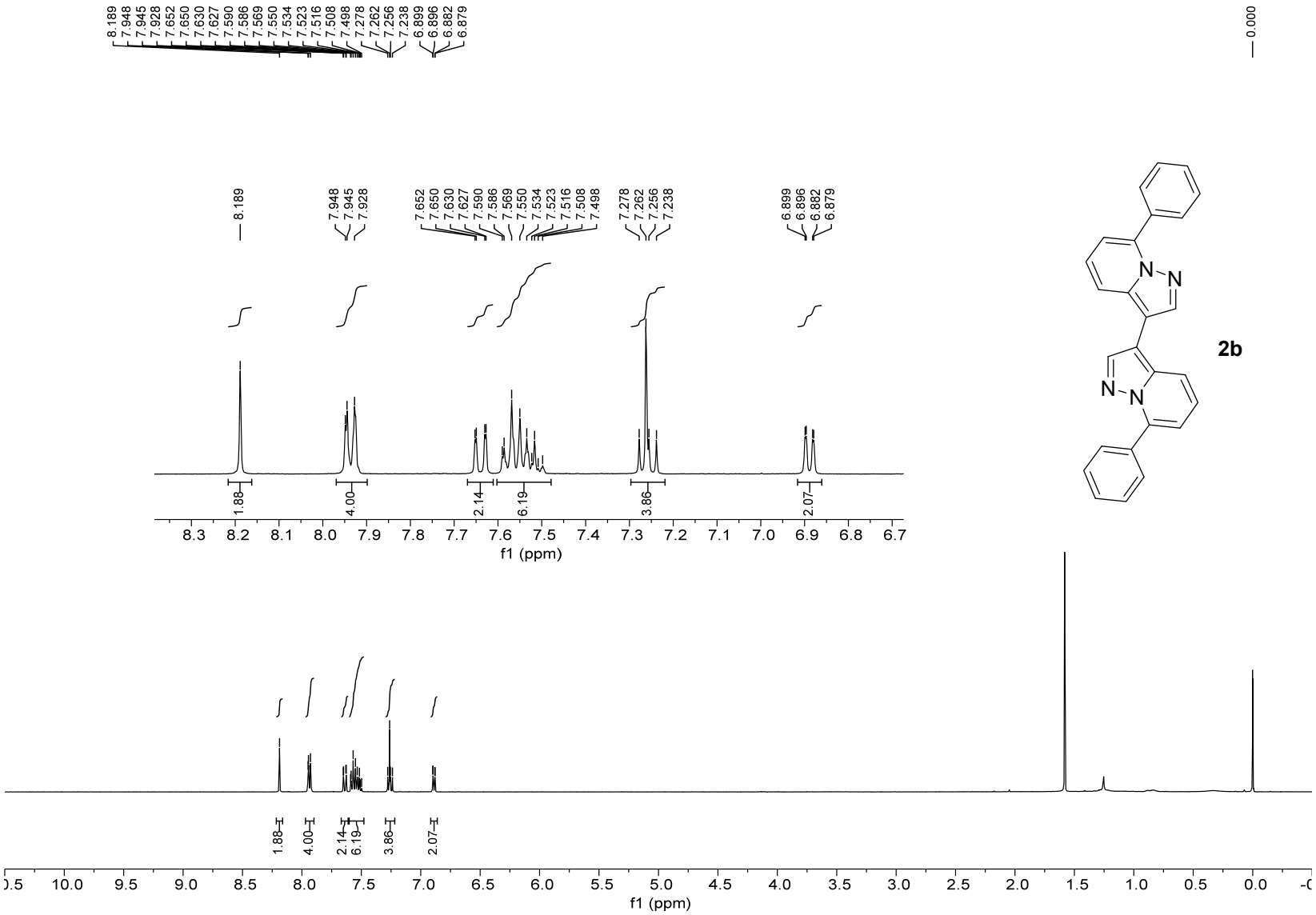

Figure S23. ^{1}H NMR spectrum of **2b** (400 MHz, $CDCl_3$).

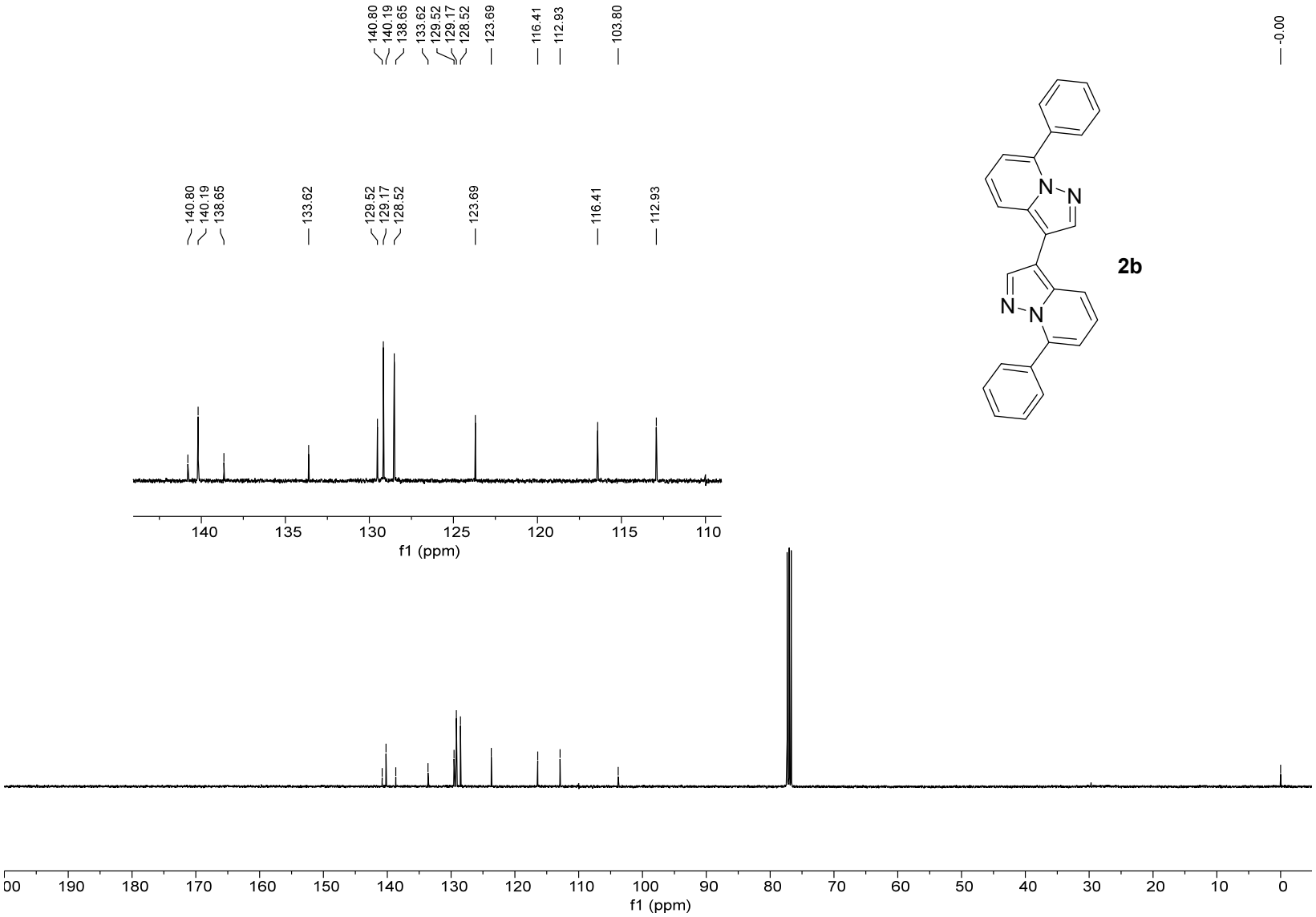

Figure S24. ^{13}C NMR spectrum of **2b** (101 MHz, $CDCl_3$).

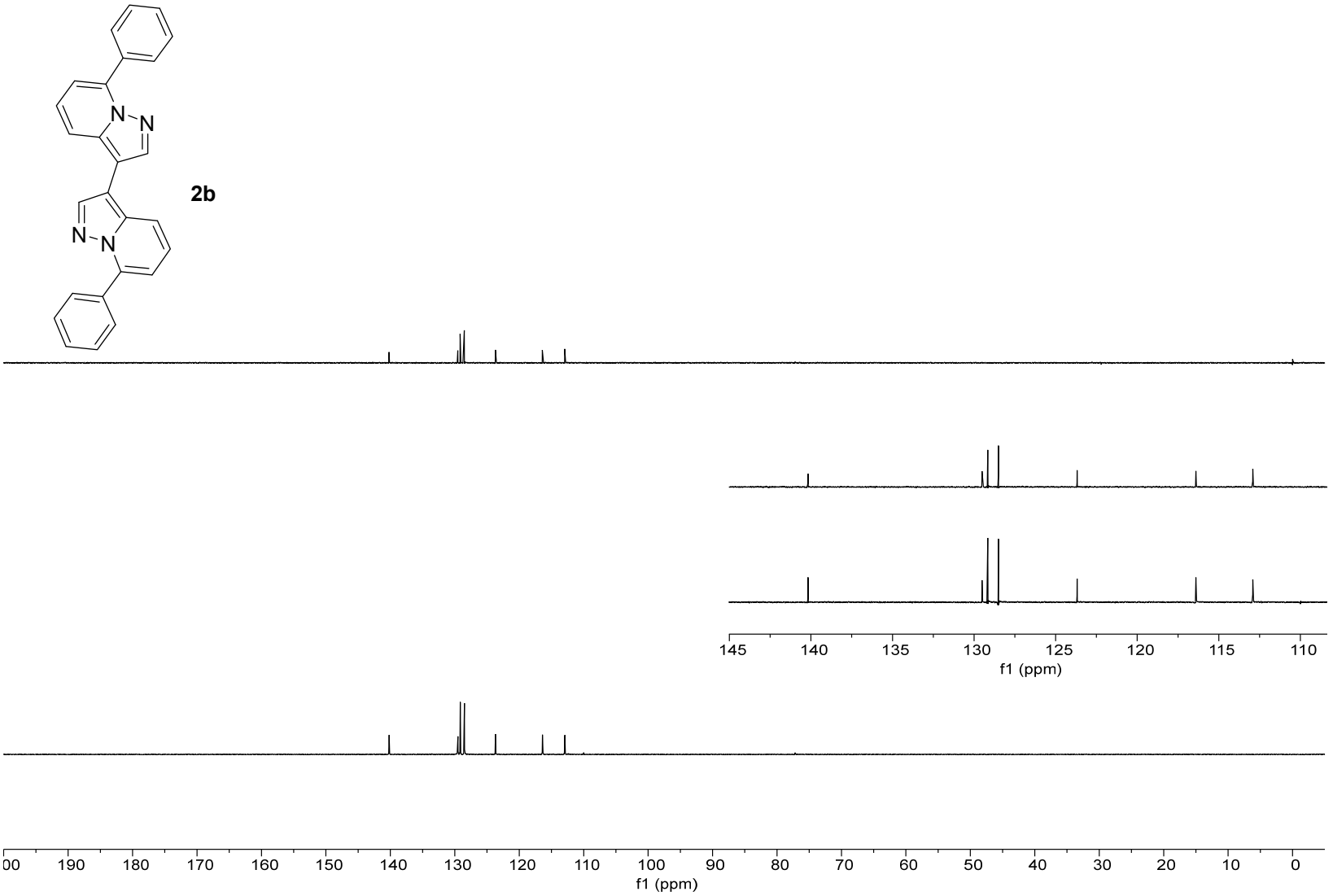

Figure S25. DEPT (90 and 135º) NMR spectra of **2b** (101 MHz, $CDCl_3$).

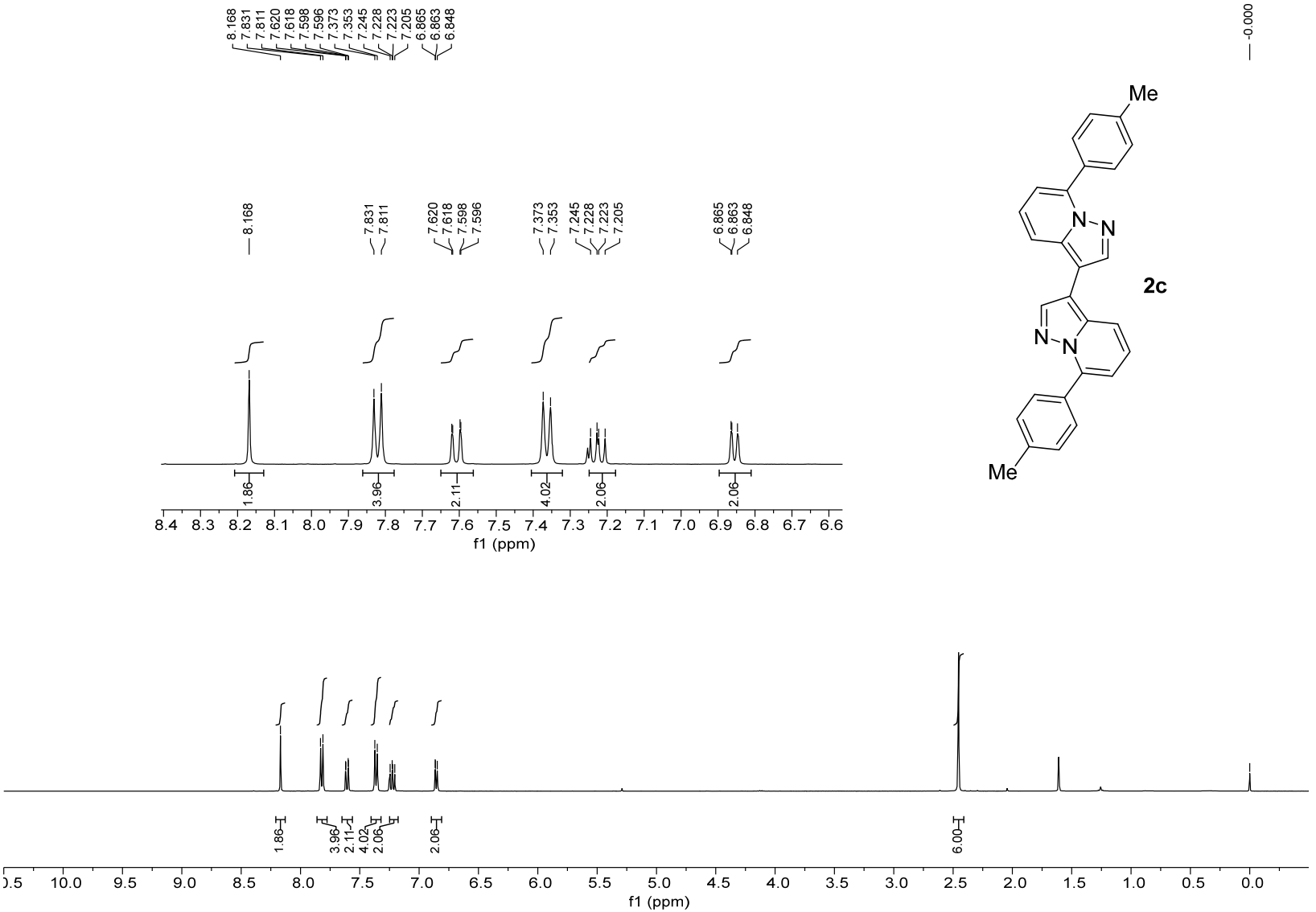

Figure S26. ^{1}H NMR spectrum of **2c** (400 MHz, $CDCl_3$).

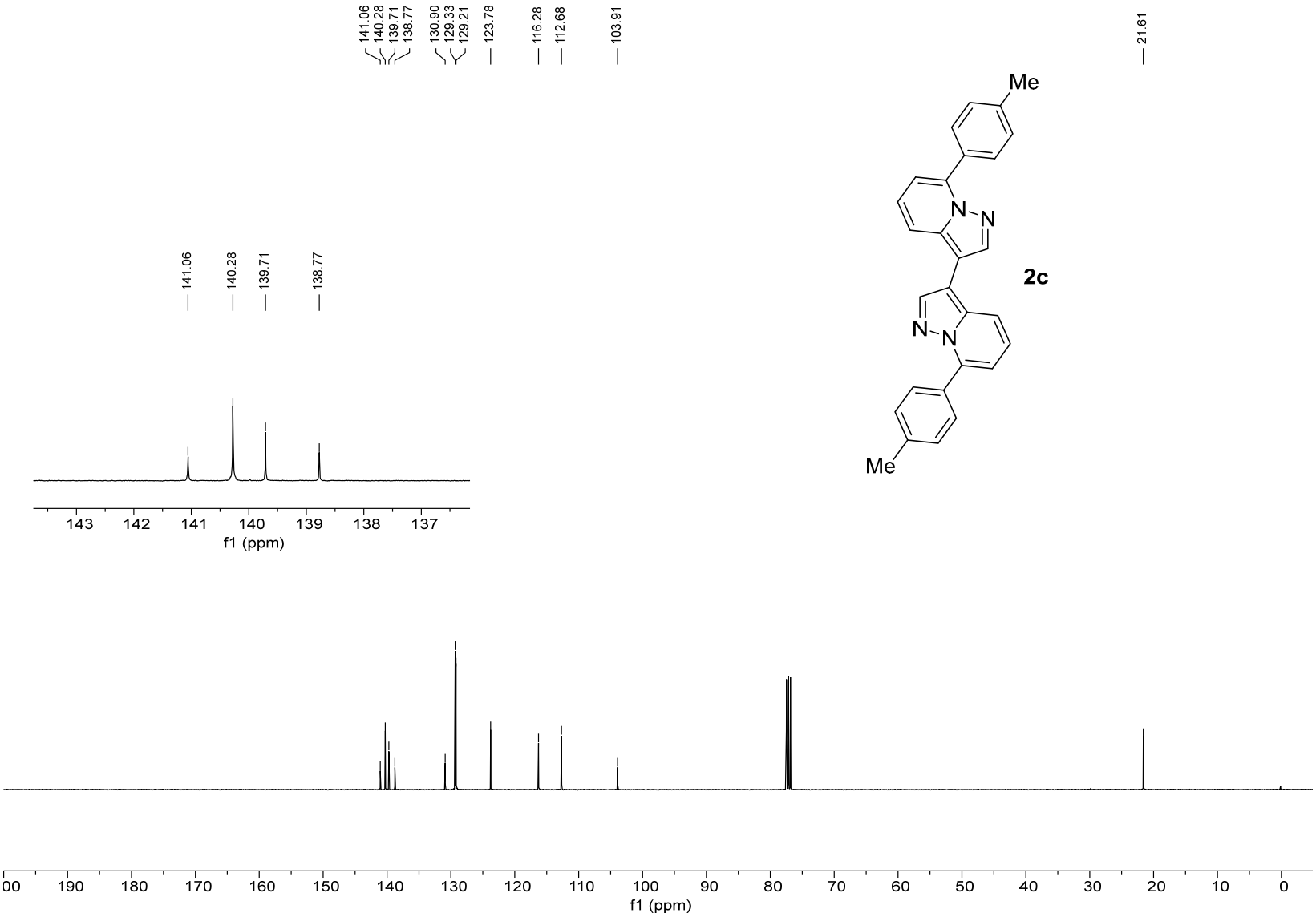

Figure S27. ^{13}C NMR spectrum of **2c** (101 MHz, $CDCl_3$).

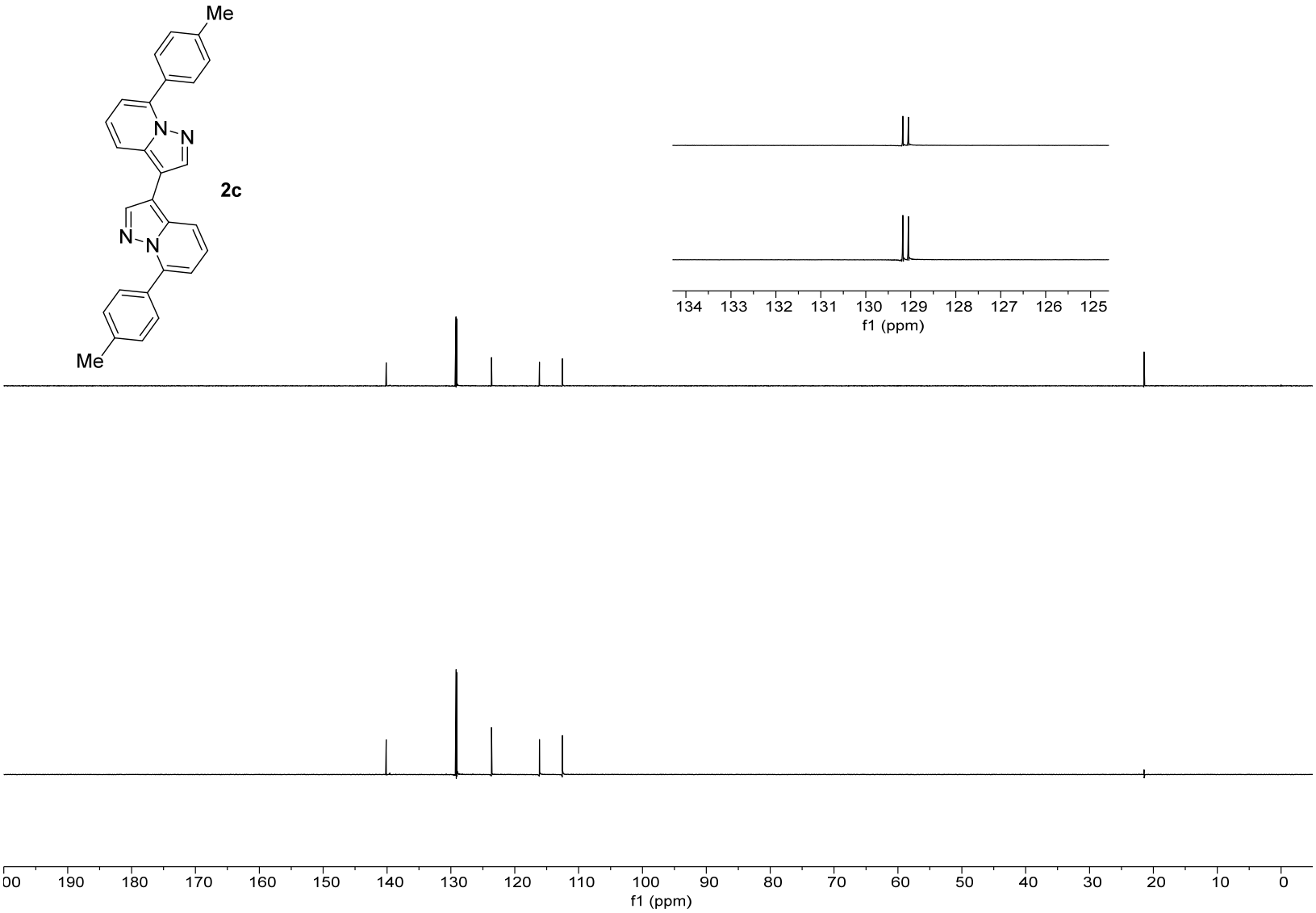

Figure S28. DEPT (90 and 135º) NMR spectra of **2c** (101 MHz, $CDCl_3$).

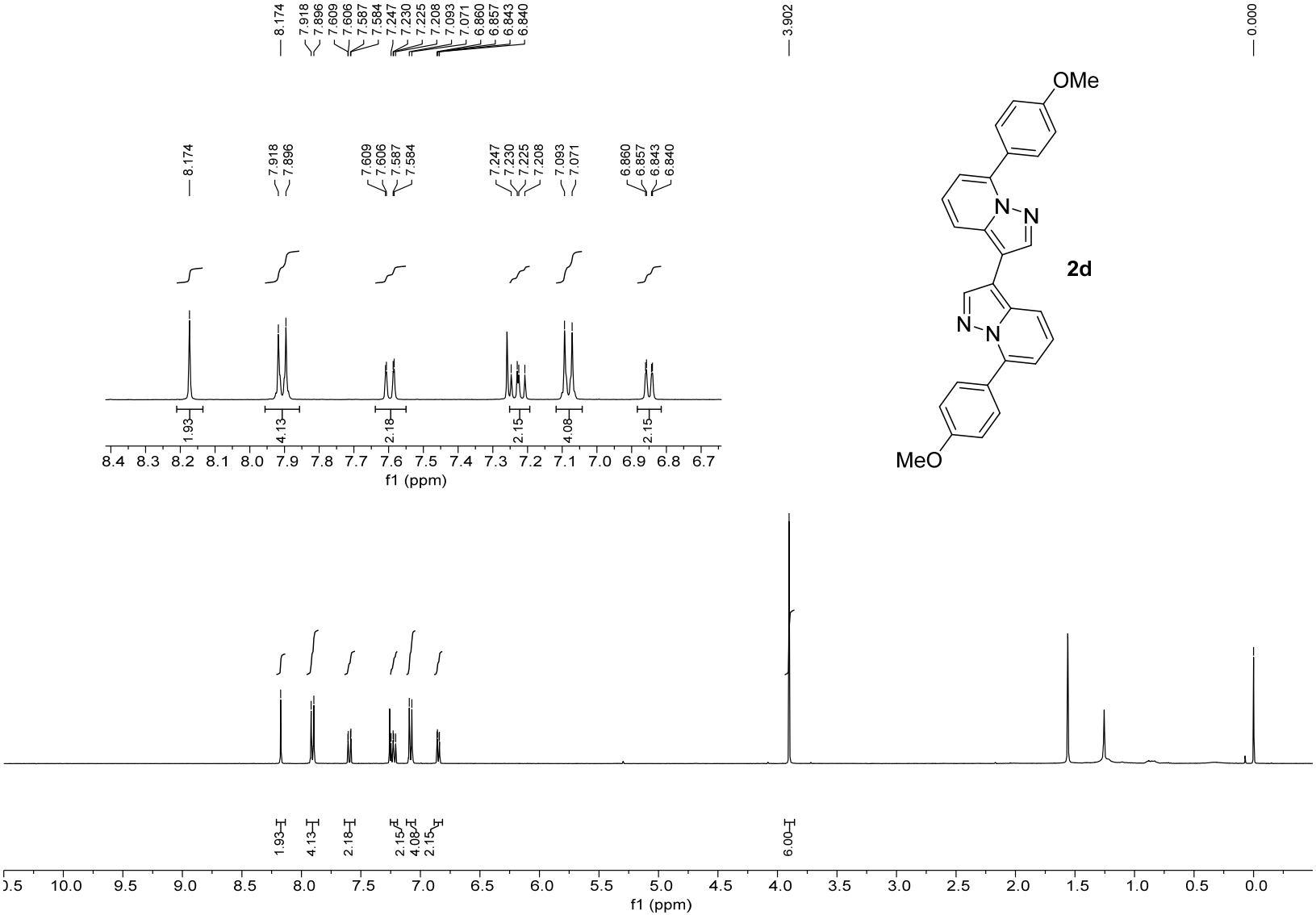

Figure S29. ^{1}H NMR spectrum of **2d** (400 MHz, $CDCl_3$).

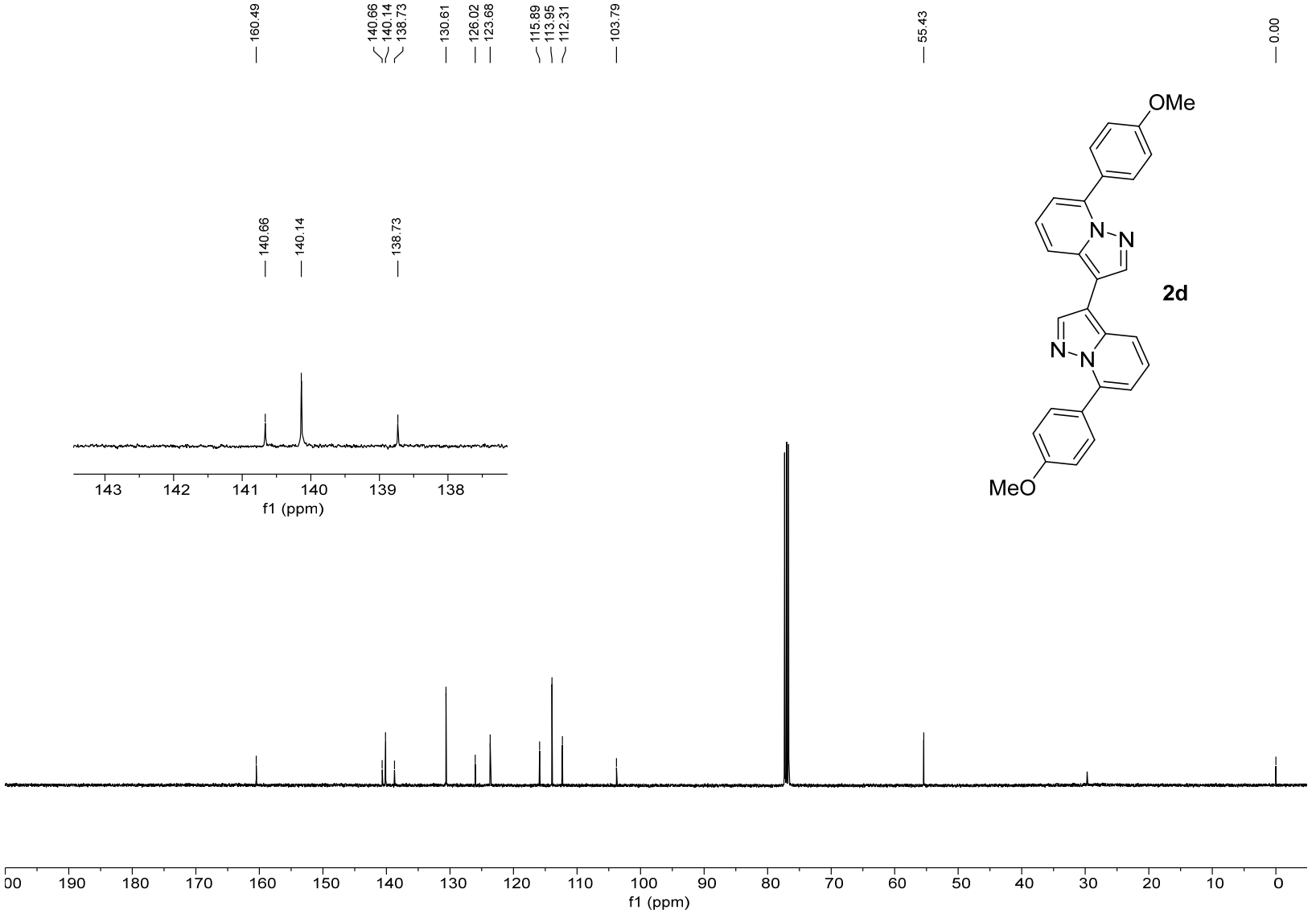

Figure S30. ^{13}C NMR spectrum of **2d** (101 MHz, $CDCl_3$).

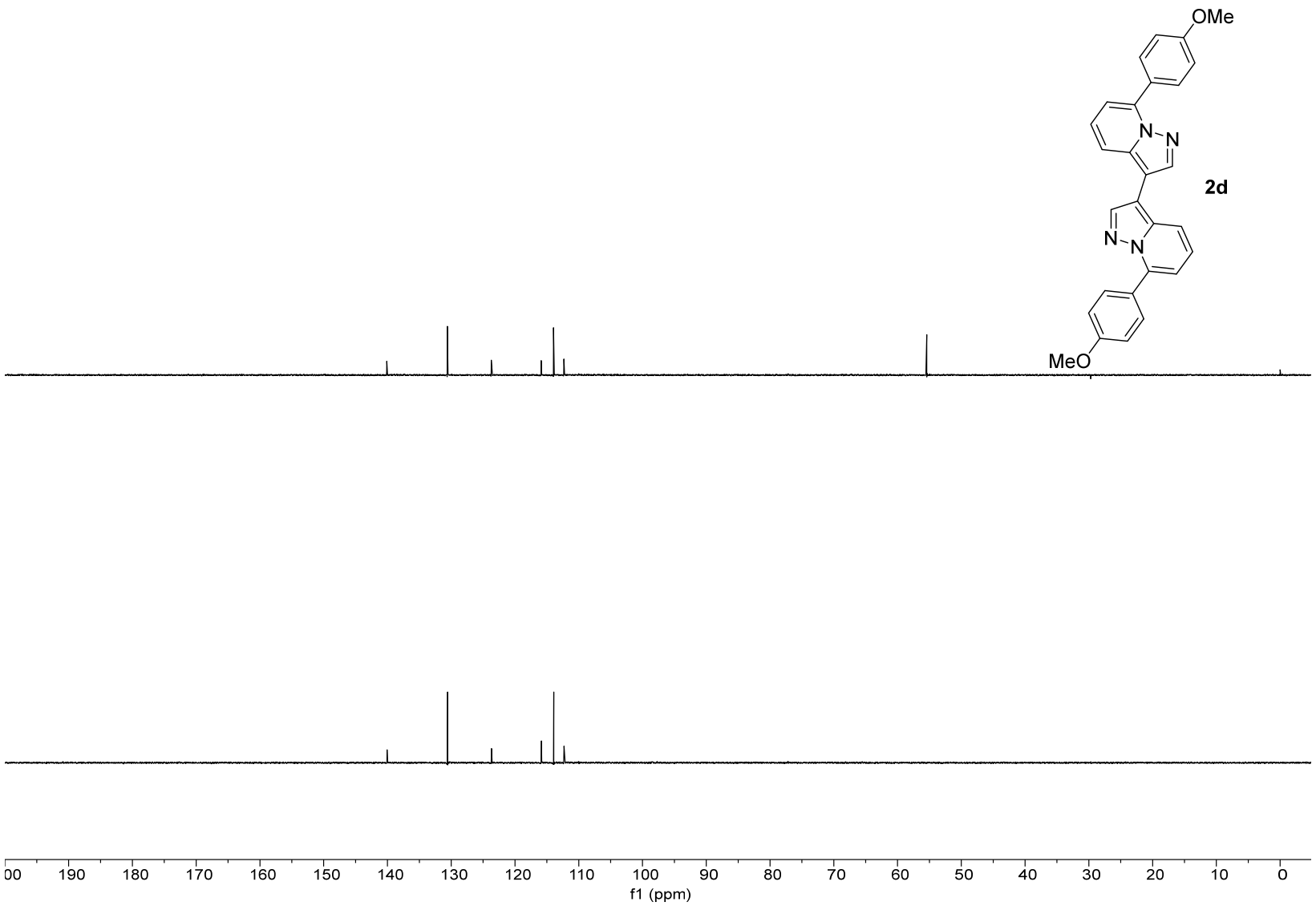

Figure S31. DEPT (90 and 135º) NMR spectra of **2d** (101 MHz, $CDCl_3$).

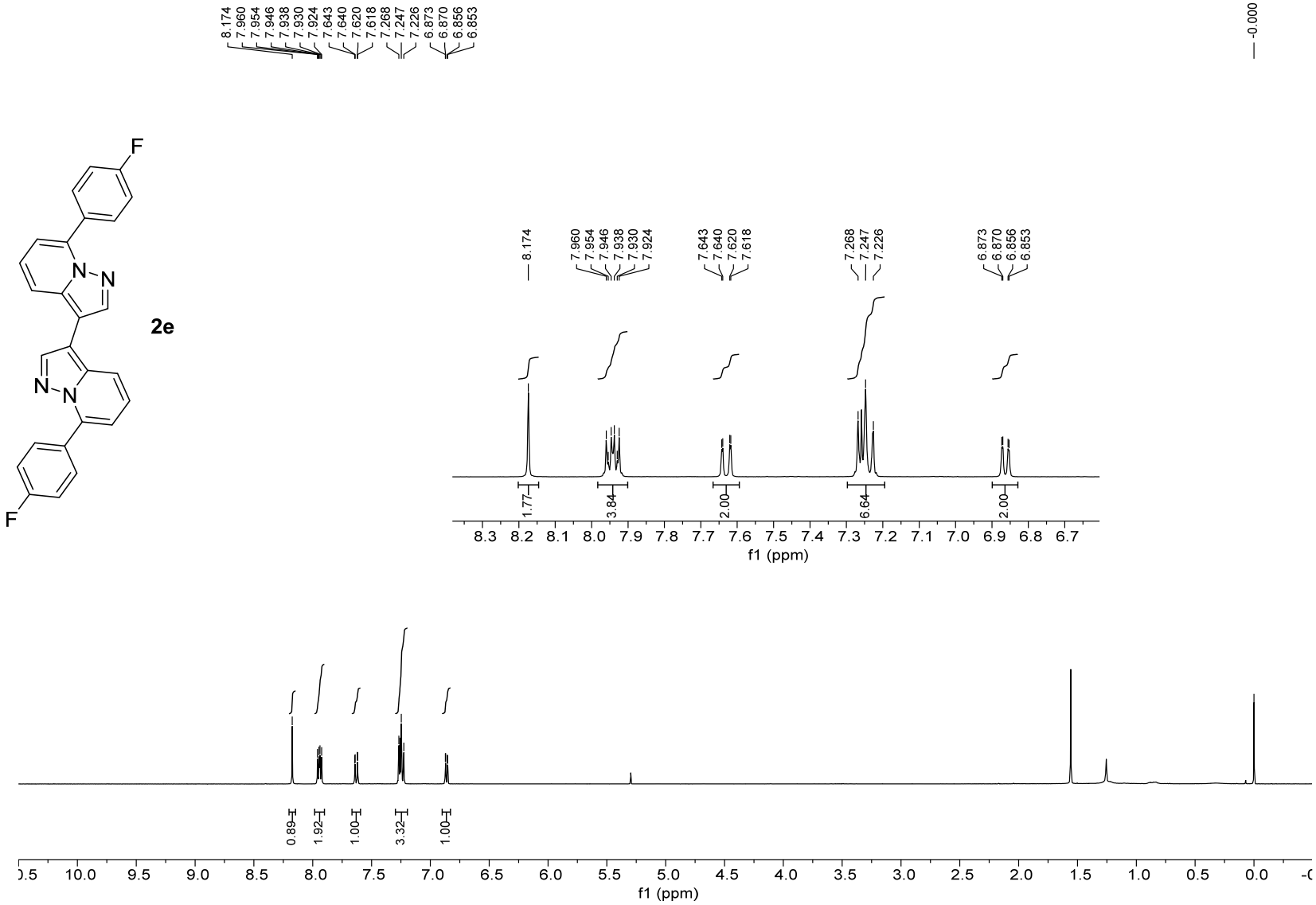

Figure S32. ^{1}H NMR spectrum of **2e** (400 MHz, $CDCl_3$).

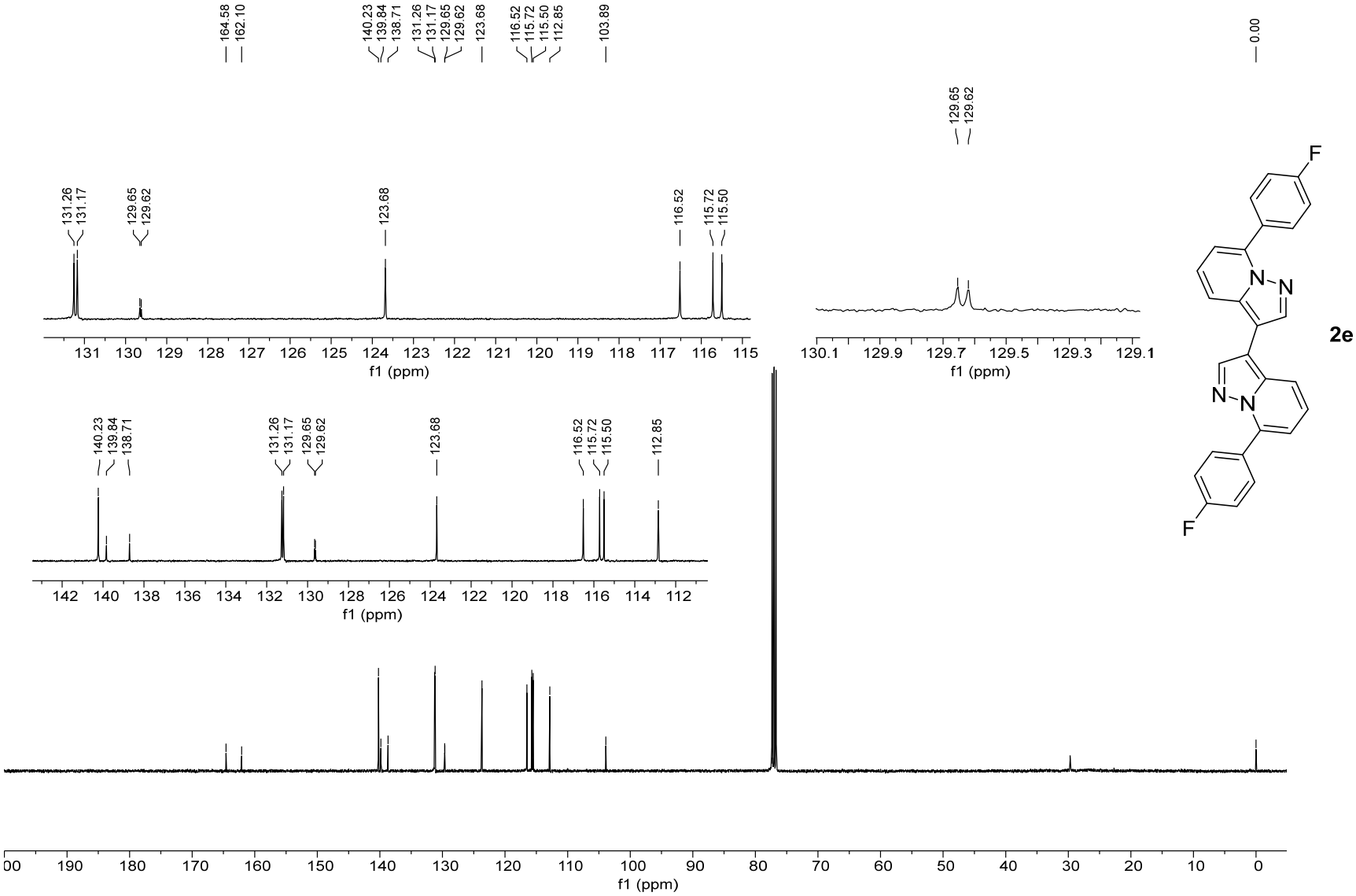

Figure S33. ^{13}C NMR spectrum of **2e** (101 MHz, $CDCl_3$).

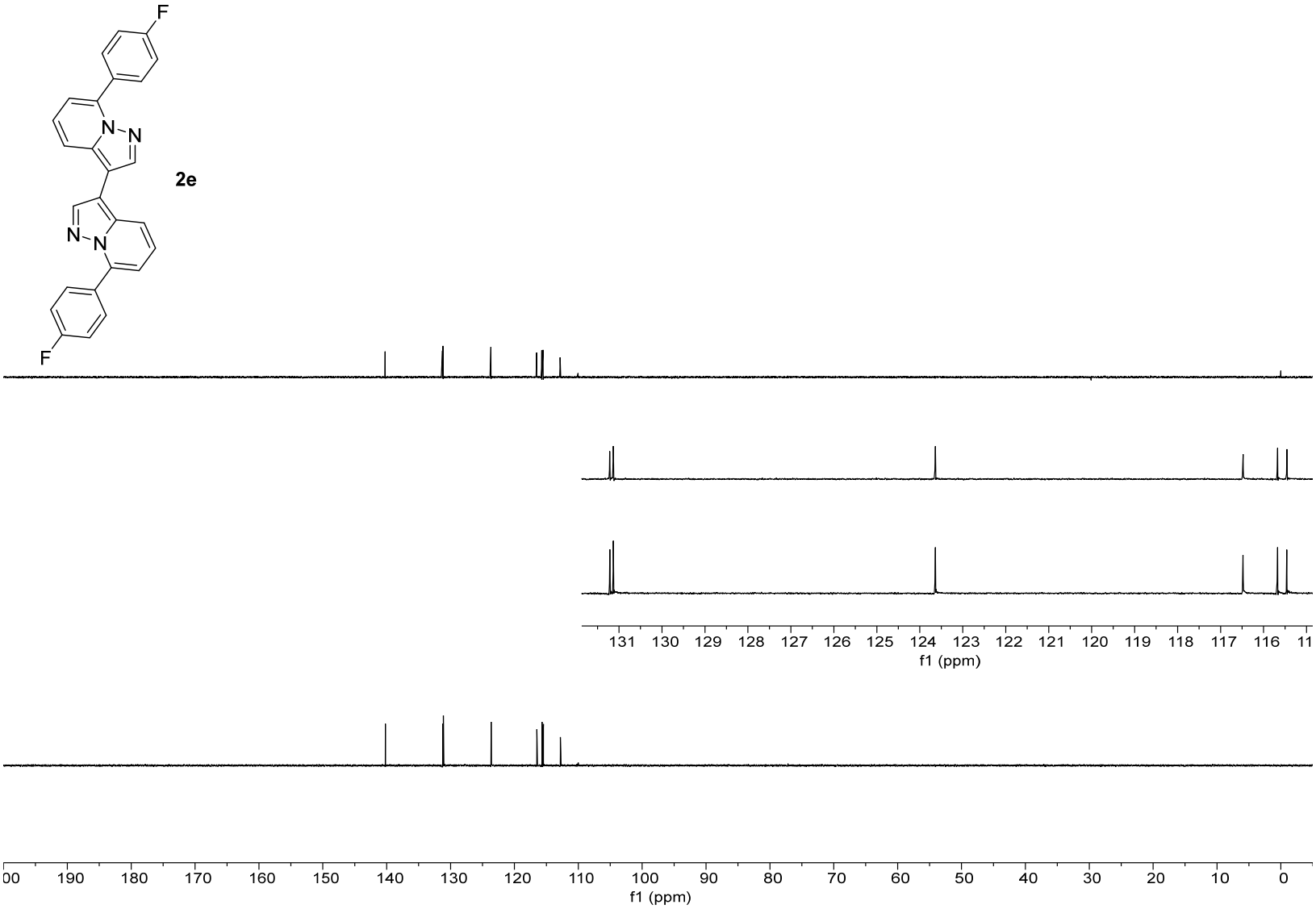

Figure S34. DEPT (90 and 135º) NMR spectra of **2e** (101 MHz, $CDCl_3$).

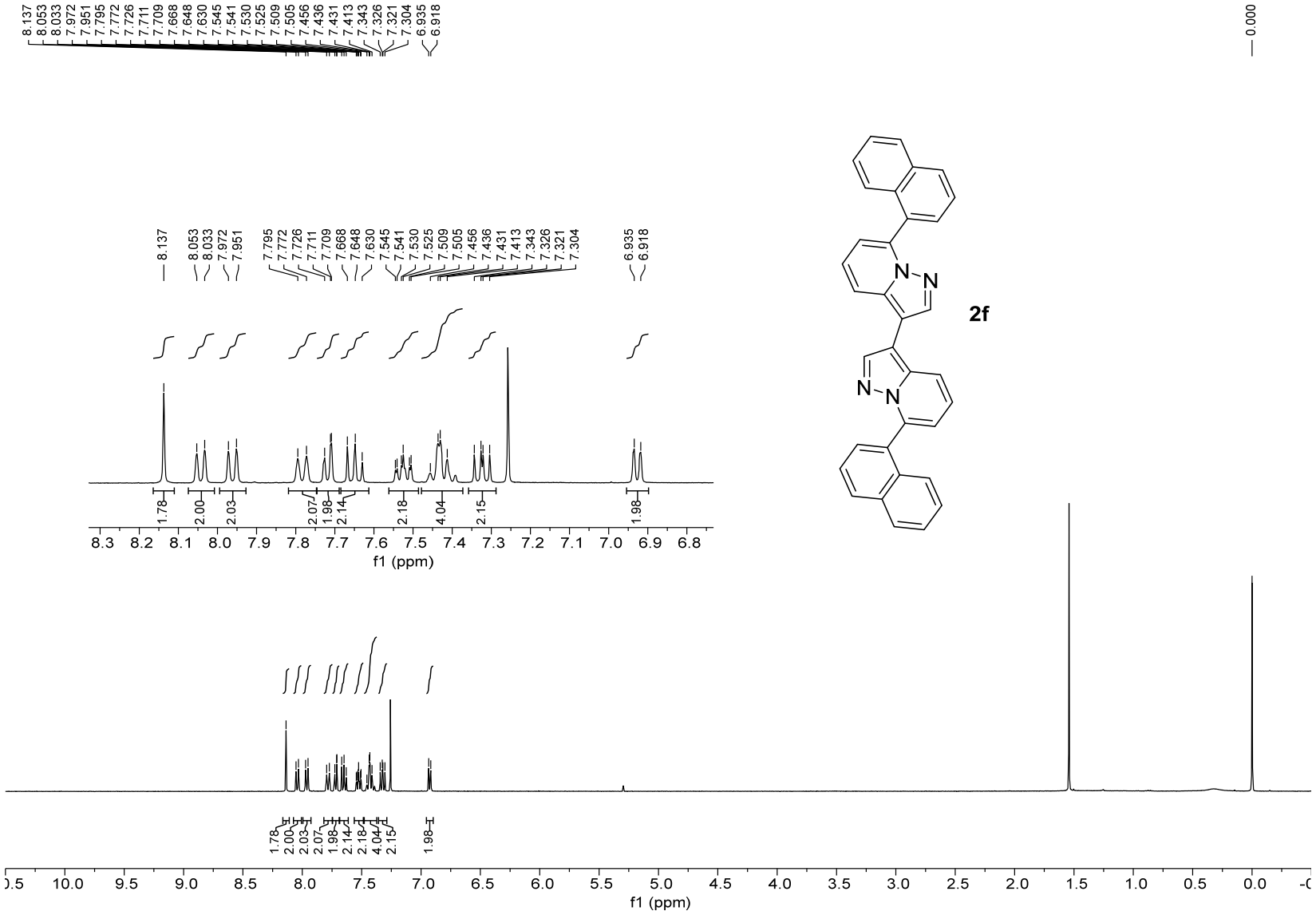

Figure S35. ^{1}H NMR spectrum of **2f** (400 MHz, $CDCl_3$).

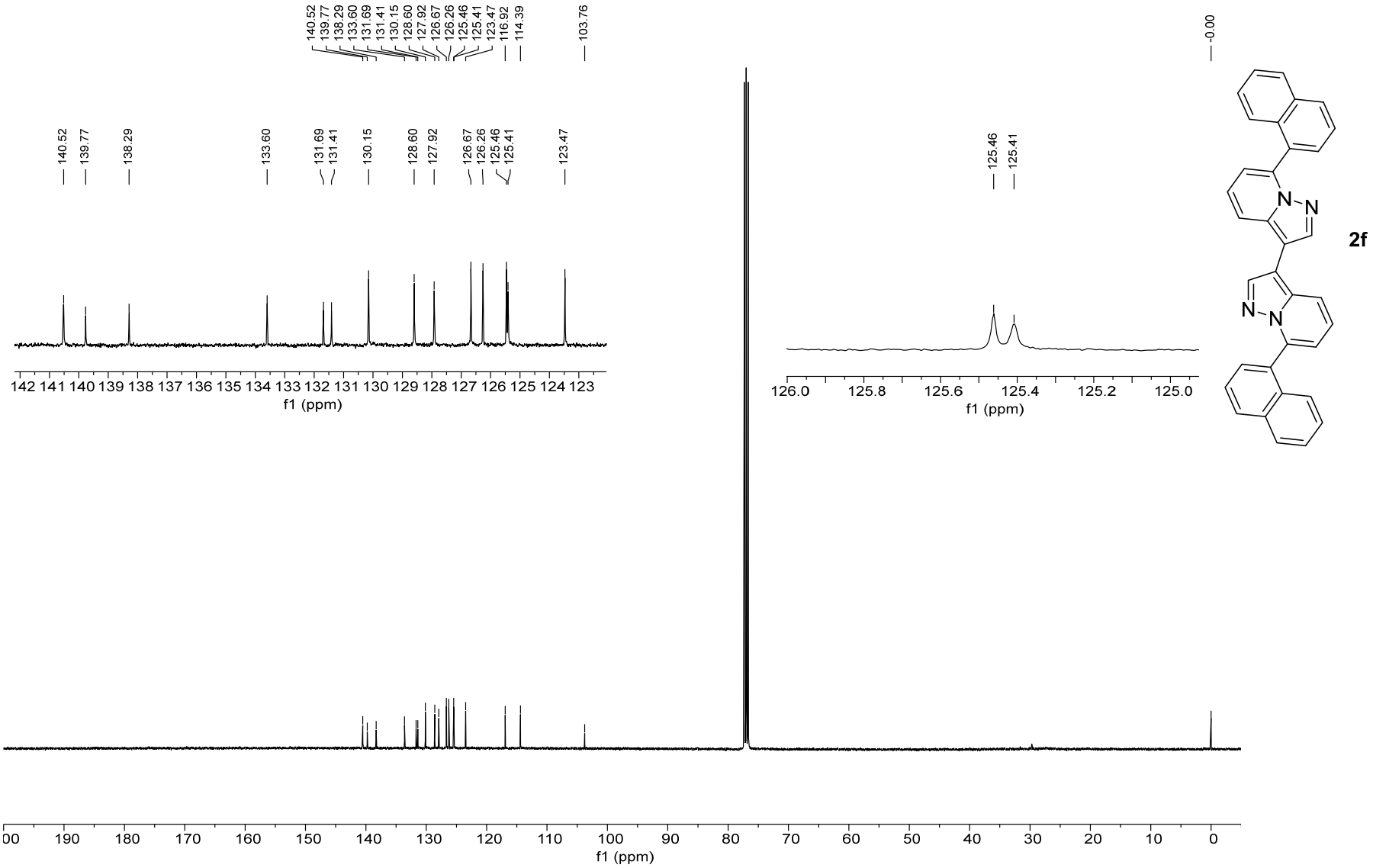

Figure S36. ^{13}C NMR spectrum of **2f** (101 MHz, $CDCl_3$).

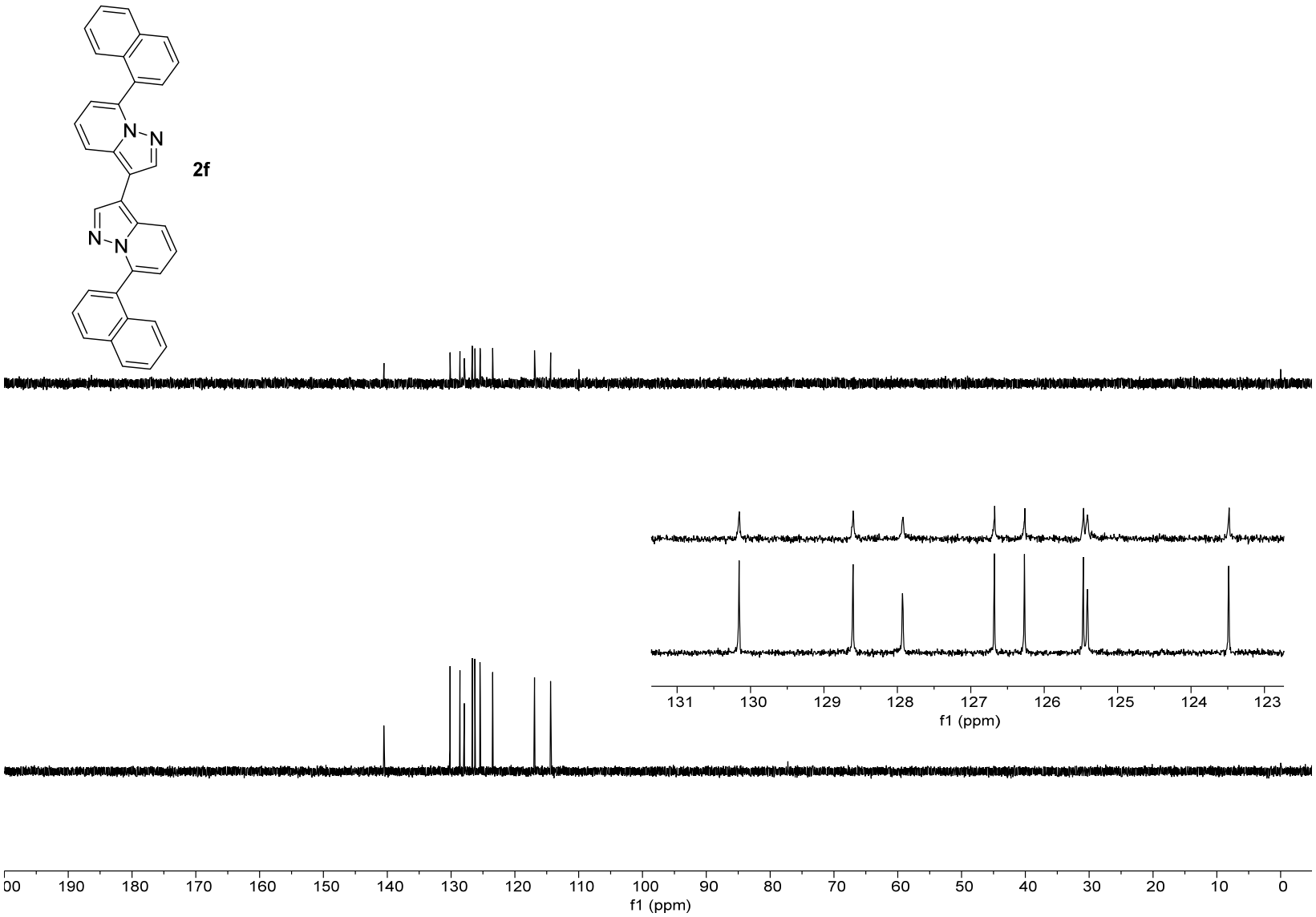

Figure S37. DEPT (90 and 135º) NMR spectra of **2f** (101 MHz, $CDCl_3$).